Accepted Manuscript

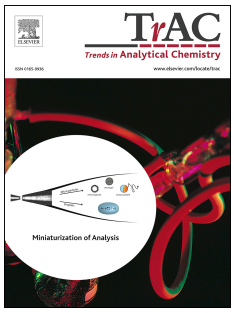

Recent development of optical methods in rapid and non-destructive detection of aflatoxin and fungal contamination in agricultural products

Feifei Tao, Haibo Yao, Zuzana Hruska, Wes Burger, Kanniah Rajasekaran, Deepak Bhatnagar

PII: S0165-9936(17)30375-8

DOI: 10.1016/j.trac.2017.12.017

Reference: TRAC 15082

To appear in: *Trends in Analytical Chemistry*

Received Date: 15 September 2017

Revised Date: 21 December 2017

Accepted Date: 22 December 2017

Please cite this article as: F. Tao, H. Yao, Z. Hruska, W. Burger, K. Rajasekaran, D. Bhatnagar, Recent development of optical methods in rapid and non-destructive detection of aflatoxin and fungal contamination in agricultural products, *Trends in Analytical Chemistry* (2018), doi: 10.1016/j.trac.2017.12.017.

Recent development of optical methods in rapid and non-destructive detection of aflatoxin and fungal contamination in agricultural products

Feifei Tao [a], Haibo Yao [a, *], Zuzana Hruska [a], Wes Burger [a], Kanniah Rajasekaran [b], Deepak Bhatnagar [b]

[a] Geosystems Research Institute, Mississippi State University

Building 1021, Stennis Space Center, MS 39529, USA

[b] USDA-ARS, Southern Regional Research Center, New Orleans, LA 70124, USA

[*]Corresponding author:

Haibo Yao

Geosystems Research Institute, Mississippi State University

1021 Balch Blvd., Stennis Space Center, MS 39529

E-mail: haibo@gri.msstate.edu

Phone: +1-228-688-3742

Abstract

The demand for developing rapid and non-destructive techniques that is suitable to real-time and on-line detection of aflatoxin and fungal contamination has received significant attentions. Measurement techniques based on fluorescence spectroscopy (FS), near-infrared spectroscopy (NIRS) and hyperspectral imaging (HSI) have provided interesting and promising results for detecting aflatoxin and/or fungal contamination in a variety of foods. As such, the main goal of this article is to give an overview of the current research progress of FS, NIRS and HSI techniques in rapid detection of aflatoxin and fungal contamination in different varieties of agricultural products. These techniques are described in terms of their working principles, features and application advantages in detecting aflatoxins and fungal contamination. The research advances of each technique applied in different agricultural products are reviewed and the results obtained from different studies are compared and discussed. Perspectives on their future trends and challenges are also addressed.

Keywords: aflatoxin; aflatoxigenic fungus; fluorescence; near-infrared spectroscopy; hyperspectral imaging; rapid and non-destructive detection

Abbreviations

A., *Aspergillus*; AFB_1, aflatoxin B_1; AFB_2, aflatoxin B_2; AFG_1, aflatoxin G_1; AFG_2, aflatoxin G_2; ANN, artificial neural network; AOAC, Association of Analytical Communities; ARS, Agricultural Research Service; ASTM, American Society of Testing and Materials; BGYF, bright greenish yellow fluorescence; BY, bright-yellow; CDA, canonical discriminant analysis; CEN, European Committee for Standardization; CFU/cm^2, colony forming units per cm^2; COE, constant offset elimination; D, dimensional; DA, discriminant analysis; DFI, difference fluorescence index; DT, detrending; EEM, excitation-emission matrix; EF-SOSAM, enhanced spectrofluorimetry in combination with second-order standard addition method; ELISA, enzyme-linked immunosorbent assay; EU, European Union; FDA, factorial discriminant

analysis; FF, fluorescence fingerprint; FFS, forward feature selection; FS, fluorescence spectroscopy; FSP-DF, forward stepwise procedure combined with discriminant function; FT, Fourier transform; FT-NIR, Fourier transform near-infrared; FT-NIRS, Fourier transform near-infrared spectroscopy; FWHM, full width half maximum; GA, genetic algorithm; GA-SPCR, genetic algorithm combined with selective principal component regression; GA-SVM, genetic algorithm combined with support vector machine; GC, gas chromatography; HBBE, hierarchical bottleneck backward elimination; HPLC, high-performance liquid chromatography; HSI, hyperspectral imaging; IS, inoculated samples; ISO, International Organization for Standardization; KNN, *k*-nearest neighbor; LDA, linear discriminant analysis; LDB, local discriminant bases; LDB-LDA, local discriminant bases combined with linear discriminant analysis; LDC, linear discriminant classifier; LOD, limit of detection; LOGLC, logistic linear classifier; LS-SVM, least squares SVM; MAS, moving average smoothing; ML, maximum likelihood; MLP, multilayer perceptron; MLR, multiple linear regression; MMN, minimum maximum normalization; MS, multi-spectral; MSC, multiplicative scatter correction; MSI, multispectral imaging; MSU, Mississippi State University; N, normal; NDFI, normalized difference fluorescence index; NIR, near-infrared; NIRS, near-infrared spectroscopy; NN, neural network; P, purple; PARAFAC, parallel factor analysis; PARZENC, Parzen classifier; PC, principal component; PCA, principal component analysis; PCR, principal component regression; PDA, potato dextrose agar; PLS-DA, partial least squares discriminant analysis; PLSR, partial least squares regression; QDA, quadratic discriminant analysis; QDC, quadratic discriminant classifier; QHM, quantized histogram matrix; R_C, correlation coefficient of calibration set; R_C^2, determination coefficient of calibration set; R_{CV}^2, determination coefficient of cross validation; R_P, correlation coefficient of prediction set; R_P^2, determination coefficient of prediction set; REP, relative error of prediction; RF, random forest; RFE, recursive feature elimination; RFI, ratio fluorescence index; RMSD, root mean square difference; RMSECV, root mean square error of cross validation; RMSEP, root mean square error of prediction set; ROI, region of interest; RPD, residual prediction deviation; SAM, spectral angle mapper; SC, sterile control; SD, standard deviation; SECV, standard error of cross validation; SEP, standard error of prediction set; SG, Savitzky-Golay; SLS, straight line subtraction; SNR,

signal-to-noise ratio; SNV, standard normal variate; SNV-DT, SNV-detrending; SPCR, selective principal component regression; SVM, support vector machine; SWIR, short-wave infrared; TLC, thin layer chromatography; TPR, true positive rate; UC, untreated control; USDA, United Stated Department of Agriculture; UV, ultraviolet; Vis, visible; Vis/NIRS, Visible and near-infrared spectroscopy.

1. Introduction

Aflatoxins are a group of highly toxic secondary metabolites produced by fungi of the genus *Aspergillus (A.)*, predominantly *A. flavus* and *A. parasiticus* [1]. The term "aflatoxin" comes from three words, namely, *Aspergillus* genus, *flavus* species and toxin. Among the eighteen different types of aflatoxins identified to date, the naturally occurring and well-known types are aflatoxin B_1 (AFB_1, $C_{17}H_{12}O_6$), aflatoxin B_2 (AFB_2, $C_{17}H_{14}O_6$), aflatoxin G_1 (AFG_1, $C_{17}H_{12}O_7$) and aflatoxin G_2 (AFG_2, $C_{17}H_{14}O_7$) [2], with AFB_1 identified as the most common and carcinogenic one [1]. The aflatoxins are biosynthetically derived from the identical precursor (versiconal hemiacetal acetate) through the polyketide pathway [3]. Structurally, aflatoxins are a group of highly oxygenated heterocyclic difuranocoumarin compounds, containing furofuran rings, lactone rings, aromatic six-membered ring, and/or pentanone ring moiety as shown in Figure 1 [4-5].

Aflatoxins are known to be hepatotoxic, hepatocarcinogenic, teratogenic and mutagenic [6-10], and are considered as Class 1 human carcinogens by the International Agency for the Research on Cancer of the World Health Organization [11]. Among the more than 400 known mycotoxins, aflatoxins especially the AFB_1 remains the most toxic [12, 13]. However, more than 5 billion people in developing countries are reported to be chronically exposed to aflatoxins through food [14-15]. The number of deaths in Indonesia due to aflatoxin-induced liver cancer is estimated at 20,000/year [16]. Moreover, aflatoxin contamination can result in severe economic losses, *i.e.*, > $250 million in direct losses to farmers [17]. The U.S. Food and Drug Administration economists [18] estimated the annual cost of aflatoxin contamination in the United States at ~ $500 million through two categories of loss, market rejection and animal health impacts. In addition, products infected by the *Aspergillus* fungi may also contain potent hazards because

of their aflatoxin-producing character. However, aflatoxin contamination and fungal infection can occur with greater prevalence in tropical and humid climates in a wide variety of agricultural products during both the pre-harvest and post-harvest periods. In the field, high temperature, prolonged drought conditions and high insect activities are significant factors for pre-harvest aflatoxin contamination. Warm temperature and high humidity are contributing factors that increase the fungal invasion and toxin production during post-harvest stages including storage, processing, transportation and sale [19]. Thus, efficiently detecting, identifying and separating the samples that are contaminated with aflatoxins and/or fungi is of great importance in order to reduce the risk of aflatoxins entering the food chain.

Various methods have been developed and utilized to determine aflatoxin and fungal contamination in foods. For aflatoxin detection, the available techniques include thin layer chromatography (TLC), gas chromatography (GC), high-performance liquid chromatography (HPLC), enzyme-linked immunosorbent assay (ELISA), fluorescence polarization assays, radio immunoassays, etc. [20-24]. The current analytical methods validated by the Association of Analytical Communities (AOAC), European Committee for Standardization (CEN) and International Organization for Standardization (ISO) for aflatoxins detection in agricultural and food products are mainly based on these methods mentioned above [11, 25]. Traditionally, fungal contamination in foods is determined using microbiological methods in a laboratory setting, which includes fungal enumerating using plate-counting or direct plating techniques, isolating in appropriate media and identifying the genus and species level by morphological characterization, including macroscopic characteristics (color, size, colony appearance) and microscopic characteristics (conidia, conidiophore, conidial heads) [26-28]. These methods for determining aflatoxin and fungal contamination may give accurate results in laboratories, however, most of them require skilled personnel and a well-equipped laboratory. They are also expensive, time-consuming and destructive to the test samples, making them impossible for large-scale non-destructive screening detection or integration in an on-line sorting and production system. In addition, the uneven presence of aflatoxins in both agricultural products and crops often makes the traditional sample-based analysis give a limited view of the degree of

contamination. In this context, the demand for developing a rapid and non-destructive method for sensing aflatoxin and/or fungal contamination that is suitable to real-time and on-line detection has received significant attentions.

Among currently emerging technologies, the optical-based methods have been reported to show great potential for on-line applications [29-30]. The measurement techniques based on fluorescence spectroscopy (FS), near-infrared spectroscopy (NIRS) and hyperspectral imaging (HSI) have provided interesting and promising results for detection of aflatoxin and fungal contamination in varieties of foods. Therefore, the main goal of this article is to give an overview of the current research progress in the application of FS, NIRS and HSI techniques in rapid and non-destructive detection of aflatoxin and fungal contamination in different varieties of agricultural products, which consist of corn, rice, wheat, peanuts, almond kernels, pistachio nuts, dried figs, date fruit and chili peppers., etc. These techniques are described in terms of their working principles, features and application advantages in detection of aflatoxin and/or fungal contamination. The research advances of each technique applied in a wide variety of agricultural products are reviewed and the factors influencing their qualitative and quantitative results are discussed. In addition, perspectives on their future trends and challenges are also discussed.

2. Optical techniques

2.1. Fluorescence spectroscopy

FS is an analytical technique of which the theory and methodology have been extensively exploited in the disciplines of both chemistry and biochemistry, such as in investigations of the structure, functions and reactivity of small molecules, synthetic polymers, proteins and other biological molecules, etc., however, it has just recently become a popular tool in the field of food science [31]. The applications of FS in food analysis have significantly increased during the last two decades, and it has been proven to be a useful tool for the characterization of chemical constituents, detection of hazards, and authentication analysis in varieties of foods [32].

Fluorescence is the emission of light subsequent to absorption of ultraviolet (UV) or visible (Vis) light of a fluorescent molecule or substructure, called a fluorophore. The fluorophore absorbs energy in the form of light at a specific wavelength and liberates energy in the form of emission of light at a longer wavelength [33]. The basic principles can be illustrated by a Jabłoński diagram [34]. Briefly, three steps are involved in a typical fluorescence process, namely, excitation, vibrational relaxation/internal conversion, and emission. Excitation of a susceptible molecule by an incoming light happens in femtoseconds, during which light is absorbed by the molecule, and transferred to an electronically excited state. The vibrational relaxation/internal conversion refers to the process where the molecule undergoes a transition from an upper electronically excited state to a lower one, without any radiation. The final process involves the emission of light at a longer wavelength and return of the molecule to the ground state [35].

A number of compounds emit fluorescence in the Vis spectral region when excited with UV radiation. Marsh and co-workers first reported observation of a bright greenish yellow fluorescence (BGYF) in cotton bolls infected by *A. flavus* [36], and later associated aflatoxins in cotton seeds with the BGYF in the fiber [37]. The fluorescence was reported to be produced by the reaction of peroxidases in living plants with kojic acid, which is formed by *Aspergillus* types [37]. However, its mechanisms are complex and still not quite clear now. Some researchers reported aflatoxin itself as a fluorescent substance. Cole and Cox [38] found that AFB_1 peaks at excitation wavelengths of 223, 265 and 362 nm; AFB_2 has three peaks at excitation wavelengths of 222, 265 and 363 nm; AFG_1 peaks at excitation wavelengths of 243, 257, 264 and 362 nm; and AFG_2 peaks at excitation wavelengths of 214, 265 and 363 nm. With aflatoxin irradiated under UV light, the fluorescence phenomenon can occur, and particularly the two major groups, AFB and AFG can emit fluorescence in the bright-blue (425-480 nm) and blue-green (480-500 nm) spectral ranges, respectively, which makes it possible to detect aflatoxin contamination using fluorescence characteristics [39]. Actually, the currently used VICAM AflaTest method for aflatoxins detection is based on their fluorescent characteristics. However, the direct use of fluorescence spectra in agricultural

products is made difficult by the complexity of background food matrices as they may contain a great variety of natural fluorescent compounds that can overlap with the analyte signal. Currently, with the extensive investigations concerning detecting aflatoxins using FS in combination with different chemometric techniques, this technique seems to be one of the most promising non-destructive optical detection methods for monitoring aflatoxin contamination in agricultural products.

2.2. Near-infrared spectroscopy

Near-infrared (NIR) region in the electromagnetic spectrum is defined to be from 780 to 2526 nm (12821-3959 cm^{-1}) by the American Society of Testing and Materials (ASTM), which is located between the red band of the visible light and the mid-infrared regions [40]. The NIRS detection technique is based on the principle that different chemical bonds in the tested sample absorb or emit different wavelengths of light when irradiated by continuous changing frequency of NIR light. NIR signals are associated with molecular vibrations, specifically the overtones and combinations of fundamental vibrations. Chemical bonds between light atoms, such as C-H, O-H, and N-H generally have high vibrational frequencies, which result in overtone and combination bands that are detectable in the NIR region [41].

For NIRS, there are mainly three modes of data collection, namely, reflectance, transmittance and interactance [42]. The determination of a suitable measurement mode relies on the type of sample and the constituents to be tested. Most of the studies reported on detection of aflatoxin contamination and fungal infection using NIRS employed the measurement mode of reflectance. The NIRS instruments can be categorized into three groups according to Baeten and Dardenne [43], namely, (i) sequential instruments, where the reflectance or absorbance is sequentially collected in time and the instrument is equipped with a monochromator or filters, and generally the early NIRS instruments belong to this type; (ii) Fourier transform (FT) or multiplex instruments, where several frequencies are detected simultaneously in the form of an interferogram; and (iii) multichannel instruments, where several detectors separately detect the absorbance at several wavebands.

The NIR spectra are generally complex due to highly overlapping and weak absorption bands associated with overtones and combinations of vibrational bonds, which may need chemometric assistance for spectral interpretation and analysis. With the latest development in chemometrics and computer techniques, NIRS has been extensively studied as an effective tool for qualitative and quantitative evaluation of food quality and safety attributes [44]. The capability of NIRS in detecting aflatoxin contamination and fungal infection have been investigated and proven to be useful in a wide range of agricultural products. There is a report showing that the major Fourier transform near-infrared (FT-NIR) bands associated with aflatoxin molecules include 6923 cm^{-1} (1444 nm), 5868 cm^{-1} (1704 nm), and 5789 cm^{-1} (1727 nm,), which are corresponding to C-H stretching and deformation, 1st overtone of CH_3 and 1st overtone of CH_2, respectively [45]. Also, the FT-NIR waveband over 5000-7000 cm^{-1} (1429-2000 nm) was pointed out to tend to correlate with aflatoxin concentrations, which contain combinations and overtones associated with the various functional groups of aflatoxin and the starch molecules of corn samples [46]. Regarding fungal infection detection using NIRS, the most significant bands related to fungal infection of cereals were investigated to be around 870-1200 nm, which correspond to NH in most amino acids and aromatic rings, radical structures in cell wall components, such as furanic or phenolic compounds, and could be interpreted as signs of kernel deterioration caused by fungal infection [47].

2.3. Hyperspectral imaging

HSI is a relatively new but rapidly growing technique that integrates spectroscopic and imaging techniques to provide both spectral and spatial information of the tested sample simultaneously. The term “hyperspectral imaging” originated from remote sensing studies and was first mentioned by Goetz et al. [48]. The HSI technique can be implemented in reflectance, transmission, scattering and fluorescence modes, and the images obtained, commonly called hypercubes, are three-dimensional (3-D) data cubes with two spatial dimensions and one spectral dimension, which are made up of hundreds of contiguous wavebands for each spatial pixel of the tested sample. Therefore, compared to conventional spectroscopic techniques, the added spatial dimension enables the mapping of chemical components in the tested

sample (chemical imaging), which is particularly useful for detection of unevenly distributed components, such as aflatoxin contamination and fungal infection in agricultural products.

There are generally three approaches for acquiring 3-D hypercubes (x, y, λ), namely point-scan, line-scan and area-scan methods. In the point-scan method (i.e., the whiskbroom method), a single point is scanned along two spatial dimensions (X and Y) by moving either the sample or the detector, and hyperspectral image data are accumulated pixel by pixel. The line-scan method (i.e., the push-broom method) is an extension of the point-scan method, in which a line of spatial information with a full spectral range per spatial pixel is captured sequentially to complete a volume of spatial-spectral data [49]. Different from the spatial-scan methods of point-scan and line-scan, the area-scan method (i.e., the band sequential method) is a spectral-scan method, in which a full spatial scene at each spectral band is captured sequentially to form a 3-D hypercube data. No relative movement between the sample and the detector is required for this method, and the use of multiple band-pass filters, a liquid-crystal tunable filter, or an acousto-optic tunable filter exemplifies this approach [50-51]. Among the three methods, line-scan imaging is a typical choice for online applications where the sample is moving. Lately, HSI technique is becoming increasingly important for rapid and non-destructive assessment of food quality and safety. The applications of HSI for detecting aflatoxin contamination and fungal infection started relatively recently, while considerable studies have shown its great potential in such aspects.

3. Applications of optical techniques in detection of aflatoxin and fungal contamination

With the development of optical techniques, considerable studies have been conducted and reported on using FS, NIRS and HSI to determine aflatoxin and fungal contamination in different varieties of agricultural products. Tables 1 and 2 summarized the recent publications on detection of aflatoxin and fungal contamination, respectively. It can be observed from both tables that the three optical techniques of FS, NIRS and HSI have been studied extensively and promising results have been demonstrated in detecting aflatoxin contamination or fungal infection of different varieties of agricultural products. Among that, corn is the mainly focused product, and has been studied a lot compared to other products.

The NIRS and HSI techniques have been exploited extensively in detecting both aflatoxin and fungal contamination, while the FS technique was primarily applied to detect aflatoxin contamination and the reports on using it to determine fungal infection are rare. The detailed applications of each optical technique are described in the following sections separately.

3.1. Applications of FS

3.1.1. Applications of FS in aflatoxin contamination

Not long after the report associating aflatoxins in cotton seeds with BGYF in the cotton fiber, BGYF was observed on aflatoxin-contaminated corn kernels [52-54]. Fluorescence HSI technique is a combination of fluorescence spectra and HSI techniques. Fluorescence HSI employs UV lights as the excitation sources, which is the main difference between the fluorescence and the common HSI systems. In the past decade, fluorescence HSI technique has been developed to enable the acquisition of fluorescence image data with both high spectral and spatial resolutions [55-56] and was first utilized to detect aflatoxin-contaminated corn samples by Yao et al [57]. Series of studies conducted at Mississippi State University (MSU) have shown great potential of the fluorescence HSI technique in distinguishing aflatoxin-contaminated corn kernels [58-65]. Based on the laboratory fluorescence HSI system with the excitation wavelength centered at 365 nm, Yao et al. [59] examined the relationship between fluorescence emissions of corn kernels inoculated with *A. flavus* and their aflatoxin contamination levels. A fluorescence peak shift phenomenon was found among different groups of corn kernels contaminated with different aflatoxin levels, namely, the fluorescence peak moved toward a longer wavelength in the blue region for the highly contaminated kernels and toward a shorter wavelength for healthy or slightly contaminated kernels. Additionally, a general negative correlation was observed between the aflatoxin concentrations and the fluorescence magnitudes in the blue and green spectral regions, and an adjusted multiple linear regression (MLR) model yielding a determination coefficient of calibration set (R_C^2) of 0.72 based on 74 fluorescence wavebands, which indicated a moderate capability of fluorescence HSI in quantifying aflatoxin contents in corn kernels. The discriminant analysis showed classification accuracies

between 84% and 91% when classifying the corn samples with the aflatoxin threshold of 20 or 100 µg/kg. Further, in order to reduce the data acquisition time and image space, genetic algorithm (GA) and selective principal component regression (SPCR) algorithms were performed to select the fluorescence features. The results showed that a correlation coefficient of calibration set (R_C) of 0.80 for quantifying the aflatoxin content in infected corn kernels was achieved when using 30 of the original 74 wavebands determined by GA for SPCR transformation produced, which was comparable to that (R_C=0.82) obtained using the standard principal component regression (PCR) analysis based on the whole wavebands [60]. For the two-class classifications with the aflatoxin thresholds of 20 and 100 µg/kg, the employed support vector machine (SVM) method produced validation accuracies of 87.7% and 90.5% respectively, when using 36 and 11 fluorescence wavebands selected by the GA method. The obtained accuracies were similar to those obtained using the whole spectral bands, while the image space was reduced significantly, especially with the threshold of 100 µg/kg, where only 11 wavebands were used indicating the possibility of developing a fluorescence multispectral imaging (MSI) system for aflatoxin detection on-line [61].

In addition, Yao et al. [62] applied two image pixel-based classification algorithms of maximum likelihood (ML) and binary encoding to discriminate healthy and aflatoxin-contaminated corn kernels, and obtained the same validation accuracy of 87% using both algorithms when taking 20 µg/kg of aflatoxin as the classification threshold. When 100 µg/kg was used as the classification threshold, the binary encoding algorithm achieved a validation accuracy of 88%, better than the 80% obtained using the ML algorithm. In this work, the authors also calculated three fluorescence indices between each two-band combination, namely, the normalized difference fluorescence index (NDFI), the difference fluorescence index (DFI) and the ratio fluorescence index (RFI) and found that using the NDFI at 437 and 537 nm, the maximum correlation between the corn aflatoxin concentration and the calculated index value could be achieved at -0.81, which constituted the first important step towards the development of a new aflatoxin screening method based on the simplified MSI system that is able to separate the contaminated product from the uncontaminated stream. The fluorescence peak shift phenomenon was also observed as

previously mentioned, with the mean fluorescence peak located at 467 and 481 nm for control and contaminated corn kernels when 20 µg/kg was used as the threshold, and 470 and 484 nm for control and contaminated corn kernels with 100 µg/kg as the threshold (Figure 2). Further, Yao et al. [63] also examined the capability of fluorescence HSI in distinguishing corn kernels artificially inoculated with toxigenic (AF13) and atoxigenic (AF38) strains of *A. flavus*. In this work, the authors first classified the infected corn kernels into two groups of "glowing" and "adjacent", with the "glowing" group referring to the corn kernels that exhibited fluorescence identifiable by the human eye under UV illumination, and the "adjacent" group referring to those adjacent to the glowing fluorescent kernels. Although the linear discriminant analysis (LDA) results did not show considerable potential of the fluorescence spectra in distinguishing control (uninfected), "adjacent" and "glowing" corn kernels, it did well in identifying the corn kernels inoculated with toxigenic and atoxigenic fungal strains. Using germ and endosperm sides of "adjacent" kernels, the overall classification accuracy of 100% and 71.7% was achieved, and 71.7% and 55.5% using the "glowing" kernels, respectively. Based on all the corn data, the LDA algorithm achieved the classification accuracy of 78.9% and 77.2% in grouping corn kernels with the aflatoxin threshold of 20 µg/kg, and of 94.4% and 91.7% with the aflatoxin threshold of 100 µg/kg, when using the germ and endosperm side, respectively. As demonstrated from the results above, the germ side was found more useful in identifying both the infected strain and the aflatoxin contamination level of corn kernels using fluorescence spectra. Hruska et al. [64] from the same research group at MSU, examined the fluorescence spectra differences of aflatoxin produced by the naturally infected and artificially inoculated corn ears from the same field. Results of the study indicated that when all the spectral data across all sample ears were averaged, the potential differences between corn kernels from the naturally infected, artificially inoculated and control (healthy) ears were obscured, however, spectral analysis based on the contaminated "hot" pixels of hyperspectral images showed a distinct difference between the contaminated and control ears with fluorescence peaks centered at 501 and 478 nm, respectively. Both the artificially inoculated and naturally infected corn ears had fluorescence peaks at 501 nm, which validated the

usefulness of the achieved advancements in the fluorescence HSI technique for detection of aflatoxin from naturally infected corn ears in the field.

In addition to aflatoxin detection in corn samples, studies have also been reported with aflatoxin contaminated peanuts, hazelnuts, pistachio nuts, wheat kernels, red chili pepper, et al. Chen et al. [66] reported observing the fluorescence phenomenon on peanut kernels with excitation at 365 nm. The peanut samples with skin were prepared by artificial spiking with *A. flavus* suspension and incubating for different time intervals, namely, 0, 12, 24, 36, 48 and 72 h. The authors found that the emission peak of aflatoxin-contaminated peanuts was around 450 nm, and a negative correlation existed between the fluorescence intensities and the aflatoxin contamination levels over the spectral range of 440~460 nm. The negative correlation obtained here is in accordance with that reported by Yao et al. [59] in their work with corn kernels. While the fluorescence peak location was somewhat different, the difference could be attributed to the fluorescence peak shift phenomenon resulting from the effect of different aflatoxin concentrations and background food matrices. Kalkan et al. [67] conducted an experiment using fluorescence MSI with the excitation wavelength of 365 nm to identify aflatoxin-contaminated hazelnuts, ground red chili pepper flakes, and fungi-infected hazelnuts. The samples were screened with 12 different filters, some of which were between 400-510 nm with 10 nm full width half maximum (FWHM) and others at 550 and 600 nm with 70 and 40 nm FWHM, respectively. By developing a local discriminant bases (LDB) -based feature extraction and selection algorithm for the analysis of multispectral data, the authors extracted the features which were able to achieve the highest classification accuracy from only two or three spectral bands, making the design of a simple, effective, and practical food inspection and sorting system possible. Based on the algorithm developed for the study, the classification accuracies of 92.3% and 79.2% were obtained for hazelnuts and red chili peppers, respectively. By removing the hazelnuts/peppers that were classified as aflatoxin-contaminated, the aflatoxin concentrations were decreased from 608 to 0.84 μg/kg for the tested hazelnuts and from 38.26 to 22.85 μg/kg for the tested red chili peppers. The algorithm was also proven useful in classifying hazelnut kernels infected and

uninfected by fungi, and an accuracy of 95.7% was achieved. By removing the kernels identified as infected, the aflatoxin concentration of the tested hazelnut kernels was decreased from 608 to 0.7 μg/kg.

Studies using fluorescence spectra to detect aflatoxin contamination in pistachio nuts are many. An early work was reported to use BGYF to identify aflatoxin-contaminated nuts from 46 lots of Iranian pistachio nuts and found that 7% of the pistachio shells exhibited BGYF and kernels from the fluorescent nuts contained 50% of the total aflatoxin contained in the samples [68]. Although this work does not conclude that aflatoxin is always present where BGYF exists, the results do show that the removal of pistachio nuts with fluorescing shells from a lot could significantly reduce the total concentration of aflatoxin. Farsaie et al. [69] conducted experiments aimed to clarify the fluorescence characteristics of pistachio nuts, and their results showed that, in addition to BGYF, there were at least three other categories of fluorescence evident when excited at 360 nm, which they named purple (P), normal (N), and bright-yellow (BY). An emission ratio of I_{490}/I_{420} (where I_{490} and I_{420} are the fluorescence intensity at 490 and 420 nm, respectively) was a practical method to separate the four categories of fluorescence. Based on these results, McClure and Farsaie [70] designed a dual-wavelength fluorescence photometer to measure the fluorescence of aflatoxin-contaminated pistachio nuts and subsequently developed an automatic electro-optical sorter to remove the BGYF nuts [71]. However, no report about the viability of this method at the commercial level has been published. Meanwhile, another study concluded that the analysis of pistachio nuts with fluorescent shells was not an appropriate means to find all kernels containing high concentrations of aflatoxin because of the observed non-specific nature of BGYF as a criterion for aflatoxin screening in pistachio shells [72]. Later, Hadavi [73] investigated the feasibility of using BGYF as a discriminating factor to identify the *A. flavus*-infected pistachio nuts and consequently potentially the aflatoxin-contaminated nuts, at harvest and post-harvest. Good relationships were found between the presence of BGYF and aflatoxin contamination in pistachio nuts at harvest, and samples with visible mold post-harvest. The mean aflatoxin concentration of the BGYF pistachio nuts collected from orchards was 2414.99 μg/kg, comparing to 9.86 μg/kg of the non-BGYF pistachio nuts. The author also

pointed out that in the samples where aflatoxin contamination took place after rehydration of dried nuts post-harvest, the contamination could not be characterized by BGYF because of the lack of enzymatic activity. More recently, Lunadei et al. [39] developed a fluorescence MSI system equipped with a filter wheel to collect the fluorescence images at 410, 440, 480, 520, 560, and 600 nm with the excitation wavelength of 365 nm to identify and screen aflatoxin-contaminated pistachio nuts and cashews. By performing the forward stepwise procedure with a tolerance of 0.01, the authors determined the optimum two wavelengths for BGYF detection, namely, 480 and 520 nm for pistachio nuts, and 440 and 600 nm for cashews. The results showed that the BGYF fluorescent pistachios nuts and cashews identified by their developed MSI system contained 92% and 82%, respectively, of the total nuts that were contaminated by aflatoxins.

Except from the conventional fluorescence spectra, other types of fluorescence such as fluorescence fingerprint (FF), enhanced fluorescence have also been studied to detect aflatoxin contamination in different varieties of agricultural products. FF, which is also known as excitation-emission matrix (EEM), is a series of fluorescence emission spectra acquired at consecutive excitation wavelengths [74-75]. The FF method is highly sensitive compared with conventional fluorescence measurement because the FF method is capable of acquiring all the spectral data, which consists of three-dimensional information of excitation × emission × fluorescence intensities. Fujita et al. [76] reported a study using FF with the excitation and emission wavelengths between 200 and 800 nm to detect total aflatoxins (AFB_1, AFB_2, AFG_1 and AFG_2) in nutmeg extract. The contaminated nutmeg extract samples were artificially prepared by spiking with aflatoxin standard. Based on partial least squares regression (PLSR) modeling technique, significant correlation was observed between the actual and the predicted values, with the determination coefficient (R_P^2) and standard error (SEP) of prediction set of 0.773 and 1.0 μg/L, respectively, demonstrating that FF could be a useful tool in quantitative determination of aflatoxin concentrations in food. Another method using enhanced fluorescence was reported to detect the AFB_1 concentration in wheat kernels and pistachio nuts [77-78]. The method is based on the enhanced fluorescence of AFB_1 by

β-cyclodextrin in 10% (w/w) methanol-water solution, thus it is a sample-destructive method. However, as the enhanced fluorescence spectra can achieve much more accurate results compared with conventional fluorescence spectra, it is also reviewed in this paper as a fluorescence-based alternative for aflatoxin detection in a rapid and accurate way. The determination of AFB_1 in wheat kernels was accomplished by enhanced spectrofluorimetry in combination with second-order standard addition method (EF-SOSAM) [77]. In order to accurately determine the AFB_1 content in wheat extracts, the adopted strategy combined the use of parallel factor analysis (PARAFAC) for extraction of the pure AFB_1 signal and the standard addition method. The obtained results showed that the AFB_1 values analyzed by EF-SOSAM and HPLC techniques were well correlated in the range 0-18 μg/kg, with R_C over 0.99 and limit of detection (LOD) of 0.9 μg/kg. Additionally, the results indicated that the presence of AFG_1 in wheat poses no serious interference in determining AFB_1 content with their proposed method. The determination of AFB_1 in pistachio nuts was conducted using both normal and synchronous fluorimetry in combination with several different multivariate calibration methods and derivative techniques [78]. Synchronous fluorescence spectrometry is a simple modification of the conventional fluorescence technique, and it can afford higher selectivity thanks to the narrowing of spectral bands and the simplification of spectra [79-80]. Eighteen combinational methods of fluorescence spectra type (normal and synchronous), modeling methods (MLR, PCR and PLSR) and derivative orders (0, 1 and 2) were tested and compared to find the best model for prediction of AFB_1 in pistachio nuts. The authors found that the best result was obtained using a method based on 0-order derivative synchronous fluorescence spectra in combination with MLR, which produced the root mean square difference (RMSD) and relative error of prediction (REP) of 0.328 and 4.354%, respectively, indicating the usefulness of the developed method for quantitative determination of AFB_1 in food.

Even though the FS technique has gained great success in identifying aflatoxin-contaminated samples, it needs to be noted that controversial results were also presented in some studies. As early as 1989, Wilson [81] found that the aflatoxin-contaminated corn kernels did not always exhibit BGYF due to the

insufficient amount of peroxidase in kernels. Jacks [82] stated that certain types of fungi that do not produce aflatoxin may yield kojic acid in foods and may be misclassified as aflatoxin-contaminated by the BGYF test. Atas et al. [83] also argued that lack of the peroxidase enzyme may conceal the presence of aflatoxins due to the absence of BGYF, and thus BGYF itself could not directly indicate the actual presence of aflatoxin as it may result in false positives and negatives during the evaluation stage.

3.2. Applications of NIRS

3.2.1. Applications of NIRS in detection of aflatoxin contamination

Over the last two decades, a considerable amount of studies have been reported employing the NIRS technique in either reflectance or transmittance mode to detect aflatoxin contamination in a wide variety of agricultural products, with most of them focusing on corn samples. To the best of our knowledge, Pearson et al. [84] reported the first results using NIRS to evaluate aflatoxin contamination in corn kernels where the contaminated samples were artificially prepared by wound-inoculation with *A. flavus* during the late milk to early dough stage of kernel maturity. Both the transmittance and reflectance spectra over the spectral range of 500-950 nm and 550-1700 nm were collected and applied to investigate their capabilities in distinguishing the aflatoxin contamination levels of single corn kernels. Based on both discriminant analysis (DA) and PLSR, qualitative models were established to classify the aflatoxin contamination of single corn kernels into three groups, namely, low (< 10 μg/kg), intermediate (10 to 100 μg/kg) and high (> 100 μg/kg) groups. Overall, the obtained results showed that the classification accuracies were similar when using DA or PLSR, and the classification models established using the transmittance spectra yielded slightly better results than using reflectance. In detail, more than 95% of the corn kernels were classified correctly as containing either high (> 100 μg/kg) or low (< 10 μg/kg) levels of aflatoxin, while the classification accuracies for the intermediate kernels (10 to 100 μg/kg) were only about 25%. The authors also found that using reflectance spectra, the germ-down orientation (germ facing the sensor) resulted in better PLSR classification accuracies for all groups than the germ-up orientation, which is probably because fungus generally invades the germ part of corn kernel first and thus it could be

easier to detect aflatoxin contamination from that part. Later, the same research group at the Agricultural Research Service, United Stated Department of Agriculture (ARS, USDA) developed and tested a high-speed dual-wavelength sorter for removing corn kernels contaminated with aflatoxin and fumonisin [85]. Based on the reflectance spectra of single kernels between 400 and 1700 nm, the absorbance band pair of 750 and 1200 nm was determined as the optimum pair of optical filters by performing DA analysis [86]. Using these two wavelengths, the classification accuracy of > 99% could be achieved in a laboratory setting with corn kernels stationary using the aflatoxin threshold of 100 µg/kg. The performance of the developed sorter was also tested at high speed with corn kernels fed by a vibratory feeder at a rate of 30 kg/hr/channel, and results showed that the reductions in aflatoxin averaged 82% with an initial level > 10 µg/kg in corn kernels, and 38% with an initial level < 10 µg/kg. It should be noted that even though the simple dual-wavelength sorter developed in this study could not work well in identifying corn kernels with low concentrations of aflatoxin contamination, it could screen and remove the highly contaminated corn kernels effectively in a high-speed environment. Thus, the developed sorter could be a low-cost, high-throughput, useful tool for decreasing aflatoxin contamination for big lot samples.

More recently, a similar study reported investigating the potential use of a low-cost, multispectral sorter in identifying aflatoxin- and fumonisin-contaminated Kenyan corn kernels [87]. The corn samples were collected from both, small-scale corn traders in open-air markets and inoculated maize field trials in Eastern Kenya. Based on the reflectance values at nine distinct wavelengths between 470 and 1550 nm and the classification algorithms of LDA, random forest (RF) and SVM, different qualitative models were developed using the thresholds of 1, 10 and 100 µg/kg for aflatoxin and 100, 1,000 and 10,000 µg/kg for fumonisin. The results showed that with the removal thresholds of >10 µg/kg for aflatoxin and >1000 µg/kg for fumonisin, the optimum model achieved sensitivity and specificity of 77% and 83%, respectively. Specifically, the authors pointed out that the basic circuitry is relatively inexpensive (< US$100 in components), and the throughput is modest (20 kernels/s, theoretically around 25 kg/h), making it suitable for small-scale milling applications in developing countries such as Kenya. Lee et al.

[46] reported a study using Fourier transform near-infrared spectroscopy (FT-NIRS) to classify the aflatoxin contamination levels in ground corn samples. In this study, the FT-NIR reflectance spectra were recorded with assistance of an integrating sphere, in the region of 4000~9999 cm^{-1} (1000~2500 nm) from 232 genetically and phenotypically diverse and naturally-contaminated and artificially-inoculated corn samples. Based on the pre-processed spectra by normalization, 1st derivative, 2nd derivative and deconvolution, the samples were grouped into 5 categories, namely, Group 1 for < 20 µg/kg (negative), Group 2 for 20-200 µg/kg, Group 3 for 300-450 µg/kg, Group 4 for 550-700 µg/kg, and Group 5 for > 850 µg/kg. The highest classification accuracies of 96%, 96% and 72%, were achieved using the classification algorithms of LDA, *k*-nearest neighbor (KNN), and partial least squares discriminant analysis (PLS-DA), respectively, for the external validation set. Figure 3 shows the scatter plots created by the first two canonical discriminant scores derived from normalized spectra of FT-NIRS, and it can be seen that Group 1 can be clearly separated from the highly contaminated samples using only two canonical scores. Additionally, based on the quantitative modeling methods of MLR, PCR and PLSR, models were established to also quantify the aflatoxin contamination. The obtained results showed that MLR method performed best, achieving the R_P^2 and root mean square error of prediction set (RMSEP) of 0.876 and 106 µg/kg, respectively, using the deconvoluted spectra.

In addition to corn samples, a few studies have also been reported on rice and spices. Zhang et al. [88] investigated the capability of FT-NIRS absorbance spectra over the spectral range of 10000~4000 cm^{-1} (1000~2500 nm) in quantifying AFB_1 contamination in paddy rice. Both naturally and artificially contaminated samples were covered in this study. Using the pre-processed spectra by smoothing, normalizing, baseline offset, standard normal variate (SNV), SNV-detrending (SNV-DT) and multiplicative scatter correction (MSC), different PLSR equations were established. Their modeling results were compared, and the best model achieved by the SNV-DT pre-processed spectra, with R_P^2, SEP and residual prediction deviation (RPD) of 0.85, 3.21 µg/kg and 1.97, respectively. Additionally, the authors also calculated the sensitivity of such method, which achieved 0.004 µg/kg, suggesting the great

potential of FT-NIRS in detecting aflatoxin contamination. In another work, based on NIRS with assistance of a remote reflectance fiber-optic probe over the spectral range of 1100~2000 nm, Hernández-Hierro et al. [89] quantified AFB_1 and total aflatoxins contents in naturally-contaminated red paprika powder. Based on the pre-processed spectra by MSC, SNV, detrending (DT), SNV-DT, derivative transformation and smoothing, quantitative models were established using the modified PLSR algorithm. The best cross-validation results were achieved with standard error of cross validation (SECV) of 0.2 and 0.4 μg/kg for AFB_1 and total aflatoxins, respectively. External validation was also performed with few samples, which obtained RMSEP of 0.2 and 1.2 μg/kg for AFB_1 and total aflatoxins, respectively. Tripathi and Mishra [45] also reported a study quantifying AFB_1 content in red chili powder by using FT-NIRS between 12800 and 3600 cm^{-1} (780~2500 nm), however contrary to the sample preparation methods employed in the studies above, the contaminated samples were prepared by spiking the aflatoxin free chili powder with the AFB_1 standard in methanol. Using the pre-processed spectra by straight line subtraction (SLS), constant offset elimination (COE) and minimum maximum normalization (MMN), different PLSR quantitative models were established and their modeling results were compared. The obtained results showed that the best cross validation result was achieved by using the SLS pre-processed spectra between 6900.3-4998.8 and 4902.3-3999.8 cm^{-1}, with root mean square error of cross validation (RMSECV) of 0.65%. The model performance was also verified by external validation, which achieved high correlation coefficient of prediction set (R_P) of 0.967.

In an effort to address aflatoxin detection in more than a single type of grain, Fernández-Ibañez et al. [47] exploited the possibility of establishing a general model for detecting aflatoxin in both corn and barley samples. Both grating visible and near-infrared spectroscopy (Vis/NIRS) (400-2500 nm) and FT-NIRS (9000-4000 cm^{-1}, i.e., 1112-2500 nm) instruments were employed in this work, and the contaminated samples were artificially induced by vaporization with water. The PLS discriminant equations were established with the pre-processed spectra by SNV-DT and derivatives. The best modeling results using the grating NIRS instrument were achieved with the determination coefficient of cross

validation (R_{CV}^2) and SECV of 0.80 and 0.211, 0.85 and 0.176, 0.92 and 0.142, respectively, for individual corn, barley and corn + barley samples. The R_{CV}^2 and SECV using the FT-NIRS instrument were obtained with 0.82 and 0.201, 0.84 and 0.183, 0.81 and 0.203, respectively, for individual corn, barley and corn + barley samples. This work showed that the results for the combined data set of corn + barley were comparable to those obtained for individual variety of grain, which suggested the possibility of establishing a general model for detection of aflatoxin contamination in cereal grains.

3.2.2. Applications of NIRS in fungal contamination

Although products infected by fungi do not signify a definite aflatoxin contamination, fungal infection can be an important indicator for potential hazards because of their aflatoxin-producing character. In addition, fungi-infected agricultural products are generally of low quality and may have undesirable traits, such as discoloration, reduced density, being more friable, etc. In this context, investigations using optical methods to distinguish and remove such fungi-infected samples are attracting more attentions. Around two decades ago, Hirano et al. [90] reported an early work using transmittance spectra between 500 and 1500 nm to detect internally moldy peanut kernels. In this study, moldy peanut samples were artificially prepared by inoculating the spore suspension of *A. flavus* between the two seed leaves of the kernels. The authors found that the transmittance ratios of 700/1100 nm between the internally moldy and sound peanut kernels were quite different and thus, could be used to distinguish the internally moldy peanut kernels from the sound ones even though no obvious external symptoms were noted. Additionally, a strong linear relationship was found between the transmittance ratio of 700/1100 nm and the degree of triglyceride hydrolysis in peanuts, which revealed that the changes in the NIR transmittance spectra resulted mainly from the metabolization of nutrients in peanuts caused by fungal infection. Removal tests were also conducted in this work to verify the usefulness of the developed method in reducing aflatoxin contamination of peanuts. Pearson and Wicklow [86] investigated the feasibility of several non-destructive techniques including reflectance Vis/NIRS (550~1770 nm) in identifying the fungus-infected corn kernels by *A. flavus*, *A. niger*, *Diplodia maydis*, *Fusarium graminearum*, *Fusarium verticillioides*

and *Trichoderma viride*. Samples in this study were collected from corn ears which were inoculated with one of the above-mentioned fungi in the field, containing a total of 1222 Pioneer hybrid P-3394 kernels and 1120 Farm Service hybrid FS-7111 kernels. Based on the visual characteristics of each corn kernel, the samples were first separated into three categories, namely, “extensive discoloration” of 50% or more of the kernel surface, “minor discoloration” of less than 50% of the kernel surface, and “asymptomatic”, referring to no visible kernel damage. Figure 4 shows the mean absorbance spectra of each category. This figure demonstrates obvious spectral differences among different groups, especially the differences between the “asymptomatic” group and the other two groups. Based on the stepwise discriminant analysis, 3 feature wavelengths were determined in discriminating the asymptomatic and “extensive discoloration” samples, which were the wavelength combinations of 1690, 1695 and 1700 nm, 535, 1690 and 1700 nm, 540, 780 and 1405 nm using the spectra collected from the “germ side only”, “endosperm side only” and “avg. of endosperm and germ sides”, respectively. Using these determined feature wavelengths, the classification accuracies of 97%, 98% and 98% were obtained in identifying the “asymptomatic” samples from the germ, endosperm and “avg. of endosperm and germ” sides, respectively, and correspondingly, 91%, 90% and 85% for the “extensive discoloration” samples. The authors also found that using only the absorbance values at 715 and 965 nm, good results could also be achieved in identifying the “extensive discoloration” and uninfected control samples. What is more, the authors also tried to classify the infected corn kernels by their fungal species, and the results showed that Vis/NIR reflectance spectra combined with the neural network (NN) algorithm were able to classify the infected fungal species if using the “extensive discoloration” symptoms; however, if using the “minor discoloration” symptoms, the classification results were inferior.

More recently, using the reflectance spectra between 904 and 1685 nm, Tallada et al. [91] conducted a study classifying the level of fungal damage severity on corn kernels (levels 1-4, referring to asymptomatic, mildly infected, moderately infected and severely infected, respectively) and also the infecting fungus. In total, 7 fungal species were investigated, namely, *A. flavus*, *Bipolaris zeicola*,

Diplodia maydis, *Fusarium oxysporum*, *Penicillium oxalicum*, *Penicillium funiculosum* and *Trichoderma harzianum*. Using the pre-processed spectra by mean centering and SNV, two classification algorithms of LDA and multi-layer perceptron artificial neural network (ANN) were employed to establish models, however, the results in classifying the level of severity from 1 to 4 were all inferior. Thus, the authors combined the infected samples at levels 1 and 2, 3 and 4 to represent the early stage and advanced stage infection, respectively. It was found that compared to the early stage infection (levels 1 and 2), it was generally much easier to discriminate the infected samples at an advanced stage (levels 3 and 4) from the uninfected ones. For instance, based on the LDA, an average classification accuracy of 85% was obtained in discriminating the infected samples at an advanced stage from the uninfected samples, versus an average of 77% for the early stage infection. In classifying the *A. flavus*-infected and the uninfected samples, the classification accuracies of 93%, 76% and 74% were obtained for the uninfected control, early stage and advanced stage groups, respectively, using LDA, and 81%, 86% and 68% using ANN. However, the results were not useful in identifying the *A. flavus*-infected corn kernels from those infected with other fungal species using either algorithms. Further, the NIR reflectance spectra over the spectral range of 1100~2500 nm was exploited to determine the ratio of infected corn (w/w) [92]. Both ground and whole corn kernels were used, and the infected samples were artificially prepared by inoculating with the *A. flavus* spore suspension and incubated at 37 °C for 4 days. Results showed that the PLSR models based on the ground corn performed better, with the best RPD of 5.36 and 1.74 obtained using the ground and whole corn kernels, respectively.

In addition to corn samples, Sirisomboon et al. [93] examined the possibility of using the reflectance NIRS between 950 and 1650 nm to predict the percentage of fungi-infected rice. Different from the sample preparation method in Phetkaeo et al.'s work [92], the artificially infected rice samples were prepared by simply inoculating different concentrations of *A. flavus* spore suspension, in other words, no following incubation procedure was applied. Both total fungal infection and yellow-green *Aspergillus* infection were tested in this study, however, the best R_P and SEP of PLSR models only achieved 0.71 and

28.07% in detecting total fungal infection, and 0.48 and 17.93% for yellow-green *Aspergillus* infection, respectively. Compared to Phetkaeo et al.'s work [92], the inferior results may be partly due to the relatively narrower spectral range used in the present study. On the other hand, the differences in sample preparation may be another reason for the discrepancy, as the incubation following inoculation could make the symptoms of fungal infection more apparent and easier to detect. Even though only a small number of artificially infected samples were covered in this work, the results revealed the difficulty in early detection of fungal infection. Liang et al. [94] reported a study focusing on shelled almond kernels, in which the reflectance spectra between 800 and 2500 nm were applied to discriminate infected and uninfected almonds, and the infecting fungus (*A. flavus* vs. *A. parasiticus*) as well. The samples were prepared by the following procedures: i) inoculating the spore suspension of *A. flavus*, *A. parasiticus* or sterile deionized water (uninfected control) separately, ii) incubated at 31 °C for 7 days and iii) washed with sterile deionized water containing 0.05% Tween-20 to remove conidia from the surface of infected kernels. Using the pre-processed absorbance spectra by 13-point (26 nm) Savitzky-Golay (SG) 2nd derivative filter, the backward elimination process was first performed to select the most important wavelengths, and then the canonical discriminant analysis (CDA) classifiers were developed to discriminate the infected and uninfected almonds. The best (lowest total classification error rate) and smallest (built based on the least number of wavelengths without a significantly inferior error rate) classifiers achieved the total classification error rates of 0.09% and 0.26%, respectively, using 34 and 22 selected wavelengths. Figure 5 shows the mean absorbance spectra of the infected and uninfected almond kernels. It was found that the largest differences between them seemed to occur at the lipid absorbance bands (e.g. 1210, 1720 and 1760 nm). In identifying the infected fungus, the best and smallest canonical classifiers yielded the total classification error rates of 13.2% and 14.7% using 42 and 38 selected wavelengths, respectively. The wavebands related to lipids were similarly observed to contribute significantly more than did the other bands in discriminating the infecting fungus. Both *A. flavus* and *A. parasiticus* belong to *Aspergillus* section Flavi and are phylogenetically related, so the authors deduced that the main differences between these infected almond kernels result from the differences in the

metabolism and aflatoxin biosynthesis of *A. flavus* and *A. parasiticus*. Lipids are the most abundant compounds in almond kernels (49.93%), thus any changes caused by fungal invasion and metabolism could be represented in their spectra. However, in a different work, from the Vis/NIR reflectance spectra (400~1100 and 1100~2500 nm) of mycelia and spores of *A. flavus* and *A. niger*, Phetkaeo et al. [95] found the existing spectral differences between both fungi, and concluded that it was possible to identify *Aspergillus* spp. fungi from their Vis/NIR spectra.

What is more, Durmus et al. [96] reported a work on employing FT-NIRS (780-2500 nm) with assistance of a bifurcated fiber-optic probe to detect both surface-mold and aflatoxin contaminations in dried figs. The fig samples were classified as mold- and aflatoxin-positive and -negative based on the thresholds of 4 colony forming units per cm^2 (CFU/cm^2) and 4 μg/kg (the maximum allowed limit of aflatoxin in European Union (EU) countries), respectively. Using the normalized spectra, the forward feature selection (FFS) algorithm was first employed to select the most significant features, and then based on the determined features, 5 different classifiers including a linear discriminant classifier (LDC), a logistic linear classifier (LOGLC), a quadratic discriminant classifier (QDC), a KNN classifier and a Parzen classifier (PARZENC) were conducted in this work. The obtained results showed that both LDC and LOGLC classifiers performed excellently in identifying aflatoxin and surface-mold contaminations, with no errors occurring in any classifications. The authors also analyzed the correlation between the surface-mold and aflatoxin contamination, and found that 91 of the 98 mold-positive figs have more than 4 μg/kg aflatoxin concentration (aflatoxin-positive), and 71 of the 74 mold-negative figs have aflatoxin lower than 4 μg/kg (aflatoxin-negative), which indicated a strong correlation between surface-mold and aflatoxin contaminations.

3.3. Applications of HSI technique

3.3.1. Applications of HSI technique in aflatoxin contamination

Unlike the early applications of FS and NIRS in detection of aflatoxin contamination, the application of HSI for aflatoxin detection began relatively recently. Atas et al. [83] investigated the use of HSI between

400 and 720 nm (10 nm spectral bandwidth) to detect aflatoxin in naturally contaminated ground red chili pepper flakes, in which both halogen and UV lights were used for illumination. The feature vectors of energy values at individual spectral bands, images of consecutive spectral bands and quantized histogram matrix (QHM) were extracted first, and then different feature selection methods including hierarchical bottleneck backward elimination (HBBE), Guyon's SVM-recursive feature elimination (SVM-RFE), classical Fisher discrimination power and principal component analysis (PCA) were performed to decrease the data dimensions. Based on the threshold of 10 μg/kg (the maximum allowed limit of aflatoxin for spices and herbs in EU countries), the classifiers of multilayer perceptrons (MLPs) and LDA were established separately using the selected features. The obtained results showed that among all the models developed, the best classification accuracy could be achieved with 83.26% under halogen illumination using the selected QHM features by HBBE method and the MLP classifier.

Later, a number of studies were conducted using HSI to detect aflatoxin contamination in corn kernels. Wang et al. [97] first reported a study discriminating the AFB_1 contamination levels on corn surface, in which the contaminated samples were artificially prepared by dropping different amounts of aflatoxin standard dissolved in methanol on corn surface to achieve 10, 20, 100 and 500 μg/kg contamination levels. After preforming the following procedures including extracting mean reflectance spectra from the region of interest (ROI) of each corn image, absorbance transformation, SNV pre-processing, PCA and stepwise factorial discriminant analysis (FDA) over the spectral range of 1000-2500 nm, an overall classification accuracy of 88% was obtained in the prediction set. In a follow-up study conducted by Wang et al. [98], similar data processing procedures were used over the spectral range of 400-1000 nm. Quite positive results, with an overall classification accuracy of 98%, were achieved in identifying the same AFB_1 contamination levels on corn surfaces. Both studies demonstrated the potential of HSI in detecting AFB_1 contamination on corn kernel surfaces. In subsequent studies by Wang et al. [99-100], a different sample preparation method was used. HSI over the range of 1000-2500 nm was applied to detect AFB_1 contamination from artificially inoculated corn with *A. flavus* spore suspension at an early dough stage in

the field. Wang et al. [99] found that the first two principal components (PCs) extracted from the secondary PCA, namely PC_1 and PC_2, mainly reflected the common features of corn kernels regardless whether they were healthy or fungus-infected, therefore, only the PCs from PC_3 to PC_7 were used as the inputs for the spectral angle mapper (SAM) classifier to classify the healthy and contaminated corn kernels. With two commercial corn hybrids of 'BH8740VTTP' and 'BH9051RR' included in this work, the overall classification accuracies over 92.3% were achieved using the threshold of 20 μg/kg. Wang et al. [100] also reported another study in which four commercial corn hybrids of 'BH8740VTTP', 'DKC697', 'P31G98' and 'BH9051RR' were used. Based on the five PCs from PC_4 to PC_8, the SAM classifiers yielded classification accuracies of 96.15% and 50%, 80% and 70%, 82.61% and 85.71%, 83.33% and 66.67% in identifying the AFB_1<10 μg/kg or AFB_1≥100 μg/kg kernels and the 10 μg/kg ≤AFB_1<100 μg/kg kernels for 'BH8740VTTP', 'DKC697', 'P31G98' and 'BH9051RR' corn hybrids, respectively when germ sides were placed up (towards the sensor). The corresponding classification accuracies were 96.15% and 75%, 85% and 70%, 91.3% and 71.42%, 88.88% and 50% when germ sides were placed down. It could be observed that superior model performance could be generally obtained in identifying the AFB_1<10 μg/kg or AFB_1≥100 μg/kg corn kernels compared to those with 10 μg/kg ≤AFB_1<100 μg/kg. Also, no significant differences of model performance were observed between the germs-up and germs-down placement of corn kernels.

In another study by Vis/NIR HSI over the spectral range of 400-900 nm in which the contaminated samples were prepared by inoculating the toxigenic *A. flavus* suspension artificially at an early dough/late milk stage of kernel development, Zhu et al. [101] obtained 90% overall accuracies from the germ side when taking 20 and 100 μg/kg as thresholds, separately. It was also found in this work that the gradient of the slope of the reflectance spectra over the range of 700~800 nm increased as the aflatoxin contamination level increased. When the band ratio image of 800 to 700 nm was calculated and used to identify the aflatoxin contaminated kernels, an overall identification accuracy of 80% was achieved when using 100 μg/kg as the threshold. Further, Zhu et al. [65] reported integration of fluorescence and

reflectance HSI under both UV and halogen illumination, to detect aflatoxin-contaminated corn. Both least squares SVM (LS-SVM) and KNN classifiers were employed in this work, and the results showed that individual fluorescence and reflectance image data achieved generally similar classification accuracies. Using the images collected from the germ sides, the integrated form of fluorescence and reflectance was able to produce better results than using only one type of spectra (fluorescence or reflectance), and particularly, the true positive rates (TPRs) could be improved conspicuously after the integration. The best overall prediction accuracy of 95.33% was obtained using the integrated information from the germ side of corn kernels based on the LS-SVM model and the threshold of 100 µg/kg. Moreover, the authors calculated the mean aflatoxin concentration of the prediction samples and found it to be reduced from 2662.01 µg/kg to 64.04, 87.33, and 7.59 µg/kg after removing contaminated kernels identified by fluorescence, reflectance, and integrating both, respectively, from the germ side. More recently, Chu et al. [102] reported a study using NIR HSI over the spectral range of 1000-2500 nm to detect AFB_1 contamination in corn kernels which were artificially infected by inoculating *A. flavus* suspension in the field. PCA analysis was also performed to decrease the data dimensions in this work, however, unlike the above-mentioned studies by Wang et al. [99-100] where the first several PCs were avoided for developing classifiers, the authors established the SVM classification models using the first five PCs, and obtained an overall classification accuracy of 82.50% when discriminating the corn kernels into three groups of <20 µg/kg, 20-100 µg/kg and >100 µg/kg. In addition, the authors also observed that a general correlation existed between the actual AFB_1 content of corn kernels and the first several PCs, and the R_C^2 and R_P^2 achieved with 0.77 and 0.70, respectively, with large standard deviations (SDs). Kandpal et al. [103] reported a study employing short-wave infrared (SWIR) HSI (1100-1700 nm) to discriminate different AFB_1 contamination levels on corn kernel surfaces. The contaminated samples were artificially prepared by emerging healthy kernels into four concentrations of AFB_1 solutions (10, 100, 500, and 1000 µg/kg) diluted with 100% acetonitrile for ~12 h. PLS-DA models were developed to categorize control and different levels of contaminated kernels and the overall classification accuracies of 90.7%, 92.3% and 96.9% were yielded for yellow, white and purple corns, respectively. By applying the

beta coefficient of the PLS-DA model pixel-wise to the hyperspectral images, the final contamination maps of AFB_1 for different corn varieties were generated (Figure 6), providing direct visualization for AFB_1 contamination of corn kernels that could not be obtained from conventional techniques. However, it should be noted that the concentrations of 10, 100, 500, and 1000 μg/kg were not the concentrations of AFB_1 on the corn kernels, and the actual concentrations on corn kernels were unknown in this work.

3.3.2. Applications of HSI technique in fungal contamination

Yao et al. [104] reported an early work investigating the feasibility of HSI technique between 400 and 1000 nm to differentiate five fungal species which included *A. flavus*, *A. parasiticus*, *Penicillium chrysogenum*, *Fusarium moniliforme* (*verticillioides*) and *Trichoderma viride*. Two experiments were conducted, namely, each fungus was inoculated and cultured in an individual Petri dish in experiment A, and all five fungal strains were inoculated and cultured at different positions in a single dish in experiment B. All the images were acquired at day 5 of fungal growth. Based on the classification algorithm of ML, an overall fungal classification accuracy of 97.7% was achieved in experiment A, while in experiment B the accuracy dropped to 71.5%, possibly due to the rapid growth of *Trichoderma viride* in experiment B which contaminated the spectral reflectance features of the other four isolates. Additionally, 10 optimum wavebands were determined for classification of the five fungal species using stepwise discriminant analysis, namely, 450, 458, 478, 509, 541, 572, 616, 670, 743 and 864 nm. Among them, the wavelengths of 743, 458 and 541 nm were the most useful, and using them, the five fungal species could also be separated with an acceptable accuracy. Additional work was conducted by Jin et al. [105] in which the HSI system illuminated by both halogen and UV (excitation wavelength range: 180-400 nm) lights was employed to classify toxigenic and atoxigenic strains of *A. flavus* over the spectral range of 400-1000 nm. The *Aspergillus* strains of aflatoxin-producing AF13 and three non-toxin producing AF2038, AF283 and AF38 were included in this study, and the strains were all cultured on potato dextrose agar (PDA) medium for 7 days before imaging. After performing PCA for data decorrelation and dimensionality reduction, and GA for selection of PCs based on Bhattacharya distance,

SVM classifiers were developed for classification of different *Aspergillus* strains. The results showed that under the halogen light source, the average accuracy rates of 83% and 74% were obtained in classifying toxigenic fungus pixels and the atoxigenic fungus pixels, respectively; while under the UV light source, 67% and 85% classification accuracies were attained correspondingly. The pair-wise classification accuracies between toxigenic AF13 and each atoxigenic fungal species (AF38, AF283 and AF2038) were 80%, 91% and 95%, respectively, under halogen light sources, and 75%, 97% and 99% under UV lights, respectively.

Both studies mentioned above demonstrated the capability of HSI technique in classifying fungal species and *Aspergillus* strains, and in this context, studies on early detection of fungal infection in different varieties of agricultural products were carried out and promising results were demonstrated. Fiore et al. [106] reported a study using the Vis/NIR HSI technique (400-1000 nm) to detect fungal infection of corn kernels. The authors first examined the system's feasibility in identifying fungal species inoculated with conidial suspensions on PDA medium in Petri dishes and incubated for 7 days. It was found that each species showed an increasing absorbance spectral signal during the growth. To evaluate the changes induced by fungal contamination on corn kernels in spectral profiles, artificial contamination assays with different fungal species (*A. flavus* 3357, *A. parasiticus* 2999, *A. niger* 7096 or *Fusarium graminearum* 126) were carried out with 12 commercial maize hybrids (*Z. mays* L.). The infected corn kernels were incubated for a total of 10 days, and were taken out for imaging on day1, day 2, day 3, day 4, day 7 and day 10. By performing PCA analysis, the four wavelengths of 410, 470, 535 and 945 nm were selected as taking the highest factor loadings. The authors found that for corn kernels inoculated with *A. flavus* 3357, the Fisher's least significant difference analysis of spectra between the categories of uninoculated (control) and day-2 infected corn samples already showed significant differences at 410 or 470 nm, which demonstrated the possibility of using the Vis/NIR HSI technique in discriminating fungus-infected corn kernels from uninfected kernels. Thus, the Vis/NIR HSI could provide an alternative technique for early detection of fungal infection of corn samples. More recently, another work with corn

samples was carried out by Zhao et al. [107] in which the NIR HSI technique over the spectral range of 921-2529 nm was utilized to identify fungus-infected corn kernels. The infected corn kernels were artificially infected with 10^6 spores/mL of *A. parasiticus* suspension, and incubated at 30 °C for 1-7 days. Mean reflectance spectra were first extracted from the ROIs, and different spectral pre-processing methods including SG smoothing, moving average smoothing (MAS), normalization, SNV and MSC were performed on the extracted spectra individually or in combination. The performance of different spectral pre-processing methods was compared based on the yielded SVM classification results. The obtained results showed that the spectral pre-processing method of "MAS+SNV" performed best when categorizing the kernels into four groups of control, day 1-day 2, day 3-day 4 and day 5-day 7. Based on that, the overall classification accuracies of 91.67% and 84.38% were achieved with all germ-up kernels (germs towards camera) and mixed germ-up (50%) and germ-down (50%) kernels, respectively.

In addition to corn samples, studies using the HSI technique to detect fungal infection have also been reported with date fruit, pistachio nuts, pulses and peanuts. Teena et al. [108] published a study employing NIR HSI over the region of 960-1700 nm to classify fungus-infected date fruit. In this work, the date fruit samples were treated as three groups: untreated control (UC), sterile control (SC) (surface sterilized, rinsed and dried) and inoculated samples (IS) (surface sterilized, rinsed, dried and inoculated with *A. flavus* suspension), and all the samples were imaged every 48 h after inoculation for a total of 10 days using an area-scan HSI system. By performing PCA, the top four most significant wavelengths corresponding to the highest factor loadings of the first PC, namely, 1120, 1300, 1610 and 1650 nm were first selected and then a total of 64 features (16 features from each selected wavelength) were extracted and applied to build the LDA and quadratic discriminant analysis (QDA) classifiers. The classification accuracies for IS were compared with UC and SC separately using six-class model (control, infected day 2, day 4, day 6, day 8 and day 10), two-class model (control vs infected (all stages of infection together)) and a pair-wise model (control vs each stage of infection). The mean accuracy (LDA and QDA) for discriminating the IS samples from the SC samples was 91.5%, 91.0% and 99.0% using the six-class,

two-class and pair-wise model, respectively. Similarly, the accuracy was 92.4%, 100.0% and 99.6% when identifying the IS samples from the UC samples using the six-class model, two-class model and pairwise-model, respectively. Another study reported classifying pistachio kernels infected by two different isolates of *A. flavus*, KK11 and R5, which are aflatoxin-producing and non-aflatoxin-producing fungal strains, respectively [109]. The infected samples were imaged every 24 h after inoculation for a total of 7 days by HSI over the spectral range of 900-1700 nm. Both the LDA and QDA classifiers were established in this work and their obtained results showed that the QDA performed better than the LDA. The QDA model could yield 100% classification accuracy in distinguishing healthy (control) samples from KK11 or R5 infected samples at all stages, while the classification accuracy dropped to 94.4% when considering infected fungal species. More recently, Karuppiah et al. [110] reported a work on the detection of fungal infection in five different pulses using NIR HSI between 900 and 1700 nm. The five pulses of chick peas, green peas, lentils, pinto beans and kidney beans were artificially infected with *A. flavus* and *Penicillium commune* by spraying with fungus-inoculated water, and the images of healthy and fungal-infected kernels were acquired at 2-week intervals (0, 2, 4, 6, 8 and 10 weeks from artificial inoculation). Both the LDA and QDA classifiers were established in six-way (healthy vs the five different stages of infection) and two-way (healthy vs every stage of infection) models, and the results showed that the LDA classifier could identify both types of fungal infections with 90-94% accuracy when using the six-way model, and with 98-100% accuracy when using the two-way models for all five types of pulses, The QDA classifier also showed promising results as it gave 85-90% accuracy for the six-way model and 96-100% accuracy for the two-way model. Also, the authors identified significant wavelengths from the first and second PC factor loadings for different types of pulses infected by *A. flavus* and *Penicillium commune* in this study.

Additionally, Pearson and Wicklow [86] also tested the capability of MSI in transmittance mode in identifying the fungus-infected corn kernels with “extensive discoloration” symptoms from asymptomatic kernels. They used 11 pass bands of the interference filters which were centered at 780, 830, 870, 880, 890, 905, 920, 930, 960, 980 and 1020 nm with a 10-nm full width in this work, and their results showed

that using 3 determined features determined by stepwise discriminant analysis, the classification accuracies of 93% and 90% could be achieved for asymptomatic and “extensive discoloration” groups, respectively. The 3 selected features were % 780 nm pixels < 112, % 920 nm pixels < 208, and % 1020 nm pixels < 128.

4. Conclusions and future prospects

This review summarized the recent research progress of three important optical techniques, namely FS, NIRS and HSI techniques in rapid and non-destructive detection of aflatoxin contamination and fungal infection in a wide variety of agricultural products, and promising results from the reported studies have demonstrated the capabilities of such optical-based methods. Depending on their detection principles and hardware components, each optical technique has its own characteristic properties in detecting aflatoxin and fungal contaminations. In detail, due to the specific occurrence of fluorescence phenomenon, FS can show high sensitivity and specificity when detecting aflatoxin contamination compared with the other two optical techniques. However, the background fluorescent elements from the tested sample can often affect the obtained aflatoxin fluorescence spectra, resulting in mixed wide or shifted fluorescence peaks. As a result, it seems more important to employ suitable chemometric techniques for handling fluorescence spectral data in order to obtain accurate models for detecting aflatoxins. NIRS, as a classical optical method, has shown great capabilities in detection of both aflatoxin contamination and fungal infection in different varieties of agricultural products, and some researchers even developed an automatic sorter for removing high concentrations of aflatoxin-contaminated corn kernels based on this technique. The significant reductions in average aflatoxin concentration of entire lots using NIRS technique have been verified in several studies. However, due to its nature of “point” detection and the possible inhomogeneity of aflatoxin and fungal contamination on different commodities, the accuracy of NIRS may be limited on detection of the inhomogeneous distribution of the contaminations. Thus, multi-point detection may be required for NIRS to achieve a better prediction of the overall contamination level of the test sample. In addition, it was observed from the reported studies that most of the work on aflatoxin detection using

NIRS was based on the sample preparation method of natural fungal infection or artificial inoculation of aflatoxigenic fungus, which therefore involve the processes of fungal growth and metabolic activities that may cause interior and/or external changes of the tested samples. Therefore, the underlying principle of such detections using NIRS still needs to be investigated. Other than the spectroscopic methods which are generally considered to be based on point-detection, HSI fuses the merits of traditional imaging and spectroscopy techniques, and thus enables the mapping of contaminations within the tested sample, which is especially useful for the uneven distribution of contaminants, such as aflatoxin. However, the HSI still remains an expensive technique, and it is still far from introducing industrial HSI sensor to applications in the automatic sorting lines. It appears that due to the high dimensionality of data and time constraints for image acquisition and subsequent image analyses when using the HSI technique, it would be more practical to seek the most sensitive wavebands so that MSI systems can be built. Development of more cost-effective and user-friendly MSI instrument appears to be the logical trend for real-time applications of HSI.

It is also apparent from this review that generally low levels of aflatoxin contamination and early stages of fungal infection may not be accurately detected, endeavors are still needed to improve it in the future. The substantial advancement of hardware and software of the instrumental systems may provide improved performance through increased efficiency of the detection system. Further, the development of novel chemometric techniques including extracting meaningful and relevant information from the overlapped and superimposed spectra of complex food matrices may open a new practical way for detection of aflatoxin contamination in agricultural products. The information fusion of different techniques can also be a promising way for higher predictive accuracy. Moreover, developments that make the instrument compact, and therefore portable, and provide a decent signal-to-noise ratio (SNR), will increase the applicability of the optical instruments for on-site analysis of aflatoxin and fungal contaminations of different commodities. With the development of optical hardware and chemometrics,

the optical-based method will become an alternative tool for the detection of aflatoxin and fungal contamination in agricultural products to ensure food and feed safety.

Acknowledgements

The authors gratefully acknowledge the financial support of the USDA cooperative agreement no. 58-6435-3-0121, the U. S. Agency for International Development via the Peanut Mycotoxin Innovation Laboratory at University of Georgia (Subaward No. RC710-059/4942206), and Mississippi State University Special Research Initiative Program.

References

[1] IARC, Chemical agents and related occupations, IARC Monographs on the Evaluation of Carcinogenic Risks to Humans,100F (2012) 1-599.

[2] E.G. Lizárraga-Paulín, E. Moreno-Martínez, S.P. Miranda-Castro, Aflatoxins and their impact on human and animal health: an emerging problem, in: R.G. Guevara-González (Ed.) Aflatoxins - Biochemistry and Molecular Biology, InTech, 2011, pp. 255-282.

[3] J.W. Bennett, D. Bhatnagar, P.K. Chang, The molecular genetics of aflatoxin biosynthesis, in: K.A. Powell, A. Renwick, J.F. Peberdy (Eds.), The Genus *Aspergillus*, Plenum Press, New York, 1994, pp. 51-58.

[4] S. Brechbühler, G. Büchi, G. Milne, The absolute configuration of the aflatoxins, The Journal of Organic Chemistry 32 (1967) 2641-2642.

[5] G. Büchi, D.M. Foulkes, M. Kuromo, G.F. Mitchell, R.S. Schneider, The total synthesis of racemic aflatoxin B_1, Journal of the American Chemical Society 89 (1967) 6745-6753.

[6] J.A. DiPaolo, J. Elis, H. Erwin, Teratogenic Response by Hamsters, Rats and Mice to Aflatoxin B_1, Nature 215 (1967) 638-639.

[7] M.E. Alpert, M.S.R. Hutt, G.N. Wogan, C.S. Davidson, Association between aflatoxin content of food and hepatoma frequency in Uganda, Cancer 28 (1971) 253-260.

[8] M. Peraica, B. Radic, A. Lucic, M. Pavlovic, Toxic effects of mycotoxins in humans, Bull, World

Health Organ. 77 (1999) 754-766.

[9] H.S. Hussein, J.M. Brasel, Toxicity, metabolism, and impact of mycotoxins on humans and animals, Toxicology 167 (2001) 101-134.

[10] IARC, Some traditional herbal medicines, some mycotoxins, naphthalene and styrene, IARC Monogr Eval Carcinog Risks Hum 82 (2002) 1-556.

[11] IARC, Some naturally occurring substances: food items and constituents, heterocyclic aromatic amines and mycotoxins, IARC Monographs on the evaluation of carcinogenic risks to humans 56 (1993) 1-599.

[12] R.A. Squire, Ranking animal carcinogens: a proposed regulatory approach. Science 214 (1981) 877-880.

[13] C.N. Ezekiel, M. Sulyok, D.A. Babalola, B. Warth, V.C. Ezekiel, R. Krska, Incidence and consumer awareness of toxigenic *Aspergillus* section *Flavi* and aflatoxin B_1 in peanut cake from Nigeria, Food Control 30 (2013) 596-601.

[14] C.P. Wild, Y.Y. Gong, Mycotoxins and human disease: A largely ignored global health issue, Carcinogenesis 31 (2010) 71-82.

[15] F. Wu, C. Narrod, M. Tiongco, Y. Liu, The health economics of aflatoxin: Global burden of disease, International Food Policy Research Institute (IFPRI). http://www.ifpri.org/publication/health-economics-aflatoxin, 2011(accessed 17.04.20).

[16] J.I. Pitt, Toxigenic fungi and mycotoxins, British Medical Bulletin 56 (2000) 184-192.

[17] J. Richard, G.A. Payne, Mycotoxins: Risk in Plant, Animal, and Human Systems, CAST Report 139, CAST, Ames, Iowa, 2003.

[18] P. Vardon, C. McLaughlin, C. Nardinelli, Potential economic costs of mycotoxins in the United States, in: J. Richard, G.A. Payne, (eds.) Mycotoxins: Risks in Plant, Animal, and Human Systems, CAST Task Force Report No. 139, CAST, Ames, Iowa, 2003, pp. 136-142.

[19] J.M. Wagacha, J.W. Muthomi, Mycotoxin problem in Africa: current status, implications to food safety and health and possible management strategies, International Journal of Food Microbiology

124 (2008) 1-12.

[20] N.W. Turner, S. Subrahmanyam, S.A. Piletsky, Analytical methods for determination of mycotoxins: A review, Analytica Chimica Acta 632 (2009) 168-180.

[21] A. Rahmani, S. Jinap, F. Soleimany, Qualitative and quantitative analysis of mycotoxins, Comprehensive Reviews in Food Science and Food Safety 8 (2009) 202-251.

[22] L. Xie, M. Chen, Y. Ying, Development of methods for determination of aflatoxins, Critical Reviews in Food Science and Nutrition 56 (2016) 2642-2664.

[23] C. Maragos, Fluorescence polarization immunoassay of mycotoxins: a review, Toxins 1 (2009) 196-207.

[24] E. Matabaro, N. Ishimwe, E. Uwimbabazi, B.H. Lee, Current immunoassay methods for the rapid detection of aflatoxin in milk and dairy products, Comprehensive Reviews in Food Science and Food Safety 16 (2017) 808-820.

[25] ISO 16050:2003, Foodstuffs -- Determination of aflatoxin B_1, and the total content of aflatoxins B_1, B_2, G_1 and G_2 in cereals, nuts and derived products -- High-performance liquid chromatographic method. https://www.iso.org/standard/29628.html, 2017 (accessed 06.12.17).

[26] R.A. Samson, E.S. Hoekstra, J.C. Frisvad, Introduction to food borne fungi, 7th ed., Centraalbureau voor Schimmelcucutures (CBS), Netherlands, 2004.

[27] R.A. Samson, S.B. Hong, J.C. Frisvad, Old and new concepts of species differentiation in *Aspergillus*, Medical Mycology 44 (2006) SI33-SI48.

[28] J.I. Pitt, A.D. Hocking, Fungi and food spoilage, 3rd ed., Springer, New York, 2009.

[29] S.D. Shackelford, T.L. Wheeler, M. Koohmaraie, Tenderness classification of beef: II. Design and analysis of a system to measure beef longissimus shear force under commercial processing conditions, Journal of Animal Science 77 (1999) 1474-1481.

[30] D.J. Vote, K.E. Belk, J.D. Tatum, J.A. Scanga, G.C. Smith, Online prediction of beef tenderness using a computer vision system equipped with a BeefCam module, Journal of Animal Science 81 (2003) 457-465.

[31] G.M. Strasburg, R.D. Ludescher, Theory and applications of fluorescence spectroscopy in food research, Trends in Food Science & Technology 6 (1995) 69-75.

[32] L. Lenhardt, R. Bro, I. Zeković, T. Dramićanin, M.D. Dramićanin, Fluorescence spectroscopy coupled with PARAFAC and PLSDA for characterization and classification of honey, Food Chemistry 175 (2015) 284-291.

[33] R. Karoui, C. Blecker, Fluorescence spectroscopy measurement for quality assessment of food system-a review, Food Bioprocess Technol. 4 (2011) 364-386.

[34] M. Zude, Optical methods for monitoring fresh and processed food-Basics and applications for a better understanding of non-destructive sensing, Taylor & Francis, Boca Raton, 2008.

[35] D. Reynolds, The Principles of Fluorescence, in: P. Coble, J. Lead, A. Baker, D. Reynolds, R. Spencer (Eds.), Aquatic Organic Matter Fluorescence (Cambridge Environmental Chemistry Series), Cambridge University Press, Cambridge, 2014, pp. 3-34.

[36] P.B. Marsh, K. Bollenbacher, J.P. San Antonio, G.V. Merola, Observation on certain fluorescent spots in raw cotton associated with the growth of microorganisms, Tex. Rec. Jour. 25 (1955) 1007-1016.

[37] P.B. Marsh, M.E. Simpson, R.J. Ferretti, T.C. Campbell, J. Donoso, The relation of aflatoxins in cotton seeds at harvest to fluorescence in the fiber, J. Agric. Food Chem. 17 (1969) 462-467.

[38] R.J. Cole, R.H. Cox, The Aflatoxins, in: Handbook of toxic fungal metabolites, Academic Press, Harahan, 1981, pp. 1-66.

[39] L. Lunadei, L. Ruiz-Garcia, L. Bodria, R. Guidetti, Image-based screening for the identification of bright greenish yellow fluorescence on pistachio nuts and cashews, Food Bioprocess Technol. 6 (2013) 1261-1268.

[40] D.A. Burns, E.W. Ciurczak, Handbook of Near-infrared Analysis, Revised and Expanded, 2nd ed., Marcel Dekker, Inc., New York, 2001.

[41] B.G. Osborne, T. Fearn, P.T. Hindle, Practical NIR spectroscopy with applications in food and beverage analysis, 2nd ed., Longman Scientific and Technical, Singapore, 1993.

[42] D. Wu, D.-W. Sun, Advanced applications of hyperspectral imaging technology for food quality and safety analysis and assessment: A review-Part I: Fundamentals, Innov. Food Sci. Emerg. Technol. 19 (2013) 1-14.

[43] V. Baeten, P. Dardenne, Spectroscopy: developments in instrumentation and analysis, Grasas y Aceites 53 (2002) 45-63.

[44] W.F. McClure, Review: 204 years of near infrared technology: 1800-2003, Journal of Near Infrared Spectroscopy 11 (2003) 487-518.

[45] S. Tripathi, H.N. Mishra, A rapid FT-NIR method for estimation of aflatoxin B1 in red chili powder, Food Control 20 (2009) 840-846.

[46] K.-M. Lee, J. Davis, T.J. Herrman, S.C. Murray, Y. Deng, An empirical evaluation of three vibrational spectroscopic methods for detection of aflatoxins in maize, Food Chemistry 173 (2015) 629-639.

[47] V. Fernández-Ibañez, A. Soldado, A. Martínez-Fernández, B. de la. Roza-Delgado, Application of near infrared spectroscopy for rapid detection of aflatoxin B_1 in maize and barley as analytical quality assessment, Food Chemistry 113 (2009) 629-634.

[48] A.F.H. Goetz, G. Vane, J.E. Solomon, B.N. Rock, Imaging spectroscopy for earth remote sensing, Science 228 (1985) 1147-1153.

[49] P. Martinsen, P. Schaare, M. Andrews, A versatile near infrared imaging spectrometer, J. Near Infrared Spectrosc. 7 (1999) 17-25.

[50] L.J. Denes, M. Gottlieb, B. Kaminsky, Acousto-optic tunable filters in imaging applications, Opt Eng. 37 (1997) 1262-1267.

[51] N. Gat, Real-time multi- and hyper-spectral imaging for remote sensing and machine vision: An overview. ASAE Paper No. 98-3027, ASAE paper, St. Joseph, MI, 1998.

[52] O.L. Shotwell, M.L. Goulden, C.W. Hesseltine, Aflatoxin contamination: Associated with foreign material and characteristic fluorescences in damaged corn kernels, Cereal Chem. 49 (1972) 458-465.

[53] O.L. Shotwell, M.L. Goulden, C.W. Hesseltine, Aflatoxin: Distribution in contaminated corn, Cereal Chem. 51 (1974) 492-499.

[54] D.I. Fennell, R.J. Bothast, E.B. Lillehoj, R.E. Peterson, Bright greenish-yellow fluorescence and associated fungi in white corn naturally contaminated with aflatoxin, Cereal Chem. 49 (1973) 404-414.

[55] M.S. Kim, Y.R. Chen, P.M. Mehl, Hyperspectral reflectance and fluorescence imaging system for food quality and safety, Trans ASAE. 44 (2001) 721-729.

[56] G. Zavattini, S. Vecchi, R.M. Leahy, D.J. Smith, S.R. Cherry, A hyperspectral fluorescence imaging system for biological applications, 2003 IEEE Nuclear Science Symposium Conference Record 2 (2004) 942-946.

[57] H. Yao, Z. Hruska, R.L. Brown, T.E. Cleveland, Hyperspectral bright greenish-yellow fluorescence (BGYF) imaging of aflatoxin-contaminated corn kernels, Proceedings of SPIE, Optics for Natural Resources, Agriculture, and Foods. 6381 (2006), 63810B1-63810B8.

[58] H. Yao, Z. Hruska, R. Kincaid, A. Ononye, R.L. Brown, T.E. Cleveland, Spectral Angle Mapper classification of fluorescence hyperspectral image for aflatoxin contaminated corn, in 2010 2nd Workshop on Hyperspectral Image and Signal Processing: Evolution in Remote Sensing (WHISPERS) (2010) 1-4.

[59] H. Yao, Z. Hruska, R. Kincaid, R. Brown, T. Cleveland, D. Bhatnagar, Correlation and classification of single kernel fluorescence hyperspectral data with aflatoxin concentration in corn kernels inoculated with *Aspergillus flavus* spores, Food Additives & Contaminants: Part A 27 (2010) 701-709.

[60] H. Yao, Z. Hruska, R. Kincaid, A. Ononye, R.L. Brown, D. Bhatnagar, T.E. Cleveland, Selective principal component regression analysis of fluorescence hyperspectral image to assess aflatoxin contamination in corn, in 2011 3rd Workshop on Hyperspectral Image and Signal Processing: Evolution in Remote Sensing (WHISPERS) (2011) 1-4.

[61] H. Yao, Z. Hruska, R. Kincaid, R.L. Brown, D. Bhatnagar, T.E. Cleveland, SVM-based feature

extraction and classification of aflatoxin contaminated corn using fluorescence hyperspectral data, in 2012 4th Workshop on Hyperspectral Image and Signal Processing: Evolution in Remote Sensing (WHISPERS) (2012) 1-4.

[62] H. Yao, Z. Hruska, R. Kincaid, R.L. Brown, D. Bhatnagar, T.E. Cleveland, Hyperspectral image classification and development of fluorescence index for single corn kernels infected with Aspergillus flavus, Transactions of the ASABE 56 (2013) 1977-1988.

[63] H. Yao, Z. Hruska, R. Kincaid, R.L. Brown, D. Bhatnagar, T.E. Cleveland, Detecting maize inoculated with toxigenic and atoxigenic fungal strains with fluorescence hyperspectral imagery, Biosystems Engineering 115 (2013) 125-135.

[64] Z. Hruska, H. Yao, R. Kincaid, D. Darlington, R.L. Brown, D. Bhatnagar, T.E. Cleveland, Fluorescence imaging spectroscopy (FIS) for comparing spectra from corn ears naturally and artificially infected with aflatoxin producing fungus, Journal of Food Science 78 (2013) T1313-T1320.

[65] F. Zhu, H. Yao, Z. Hruska, R. Kincaid, R. Brown, D. Bhatnagar, T. Cleveland, Integration of fluorescence and reflectance visible near-infrared (VNIR) hyperspectral images for detection of aflatoxins in corn kernels, Transactions of the ASABE 59 (2016) 785-794.

[66] W. Chen, D. Xing, W. Chen, Rapid Detection of *Aspergillus flavus* Contamination in Peanut with Novel Delayed Luminescence Spectra, Photochemistry and Photobiology 81 (2005) 1361-1365.

[67] H. Kalkan, P. Beriat, Y. Yardimci, T.C. Pearson, Detection of contaminated hazelnuts and ground red chili pepper flakes by multispectral imaging, Computers and Electronics in Agriculture 77 (2011) 28-34.

[68] J.W. Dickens, R.E. Welty, Fluorescence in pistachio nuts contaminated with aflatoxin, Journal of American Oil and Chemical Society 52 (1975) 448-450.

[69] A. Farsaie, W.F. McClure, R.J. Monroe, Development of indices for sorting Iranian pistachio nuts according to fluorescence, J. Food Sci. 43 (1977) 1550-1552.

[70] W.F. McClure, A. Farsaie, Dual-wavelength fiber-optic photometer measures fluorescence of

aflatoxin-contaminated pistachio nuts, Trans. ASAE 23 (1980) 204-207.

[71] A. Farsaie, W. McClure, R. Monroe, Design and development of an automatic electro optical sorter for removing BGY fluorescent pistachio nuts, Trans. ASAE (1981) 1372-1375 (abstract).

[72] W.E. Steiner, K. Brunschweiler, E. Leimbacher, R. Schneider, Aflatoxin and fluorescence in brazil nuts and pistachio nuts, Journal of Agriculture and Food Chemistry 40 (1992) 2453-2457.

[73] E. Hadavi, Several physical properties of aflatoxin-contaminated pistachio nuts: Application of BGY fluorescence for separation of aflatoxin-contaminated nuts, Food Additives and Contaminants 22 (2005) 1144-1153.

[74] M. Tsuta, K. Miyanoshita, T. Suzuki, S. Nakauchi, Y. Sagara, S. Sugiyama, Three-dimensional visualization of internal structural changes in soybean seeds during germination by excitation-emission matrix imaging, Transactions of the ASABE 50 (2007) 2127-2136.

[75] K. Fujita, M. Tsuta, M. Kokawa, J. Sugiyama, Detection of deoxynivalenol using fluorescence excitation-emission matrix, Food Bioprocess Technol. 3 (2010) 922-927.

[76] K. Fujita, J. Sugiyama, M. Tsuta, M. Shibata, M. Kokawa, H. Onda, T. Sagawa, Detection of aflatoxins B1, B2, G1 and G2 in nutmeg extract using fluorescence fingerprint, Food Sci. Technol. Res. 19 (2013) 539-545.

[77] J. Hashemi, G.A. Kram, N. Alizadeh, Enhanced spectrofluorimetric determination of aflatoxin B1 in wheat by second-order standard addition method, Talanta 75 (2008) 1075-1081.

[78] M. Aghamohammadi, J. Hashemi, G.A. Kram, N. Alizadeh, Enhanced synchronous spectrofluorimetric determination of aflatoxin B_1 in pistachio samples using multivariate analysis, Analytica Chimica Acta 582 (2007) 288-294.

[79] J.B.F. Lloyd, Synchronyzed excitation of fluorescence emission spectra, Nature Phys. Sci. 231 (1971) 64-65.

[80] T. Vo-Dinh, Multicomponent analysis by synchronous luminescence spectrometry, Anal. Chem. 50 (1978) 396-401.

[81] D. Wilson, Analytical method for aflatoxin in corn and peanuts, Arch. Environment Contamination

and Toxicology 18 (1989) 304-314.

[82] T. Jacks, Evaluation of kojic acid for determining heme and nonheme haloperoxidase activities spectrofluorometrically, Analytical Letters 38 (2005) 921-927.

[83] M. Atas, Y. Yardimci, A. Temizel, A new approach to aflatoxin detection in chili pepper by machine vision, Computers and Electronics in Agriculture 87 (2012) 129-141.

[84] T.C. Pearson, D.T. Wicklow, E.B. Maghirang, F. Xie, F.E. Dowell, Detecting aflatoxin in single corn kernels by transmittance and reflectance spectroscopy, Transactions of the ASAE 44 (2001) 1247-1254.

[85] T.C. Pearson, D.T. Wicklow, M.C. Pasikatan, Reduction of aflatoxin and fumonisin contamination in yellow corn by high-speed dual-wavelength sorting, Cereal Chemistry 81 (2004) 490-498.

[86] T.C. Pearson, D.T. Wicklow, Detection of corn kernels infected by fungi, Transactions of the ASABE 49 (2006) 1235-1245.

[87] M.J. Stasiewicz, T.D.O. Falade, M. Mutuma, S.K. Mutiga, J.J.W. Harvey, G. Fox, T.C. Pearson, J.W. Muthomi, R.J. Nelson, Multi-spectral kernel sorting to reduce aflatoxins and fumonisins in Kenyan maize, Food Control 78 (2017) 203-214.

[88] Q. Zhang, F. Jia, C. Liu, J. Sun, X. Zheng, Rapid detection of aflatoxin B_1 in paddy rice as analytical quality assessment by near infrared spectroscopy, Int J Agric & Biol Eng 7 (2014) 127-133.

[89] J.M. Hernández-Hierro, R.J. García-Villanova, I. Gonz ález-Martín, Potential of near infrared spectroscopy for the analysis of mycotoxins applied to naturally contaminated red paprika found in the Spanish market, Analytica Chimica Acta 622 (2008) 189-194.

[90] S. Hirano, N. Okawara, S. Narazaki, Near infra red detection of internally moldy nuts, Bioscience, Biotechnology, and Biochemistry 62 (1998) 102-107.

[91] J.G. Tallada, D.T. Wicklow, T.C. Pearson, P.R. Armstrong, Detection of Fungus-Infected Corn Kernels Using Near-Infrared Reflectance Spectroscopy and Color Imaging, Transactions of the ASABE 54 (2011) 1151-1158.

[92] T. Phetkaeo, R. Klaithin, P. Theanjumpol, K. Kunasakdakul, S. Thanapornpoonpong, S. Vearasilp, Comparison of Sample Preparation Methods on the Infected Corn Seed Detection by NIR Spectroscopy, Chiang Mai University Journal of Natural Sciences 11 (2012) 243-249.

[93] C.D. Sirisomboon, R. Putthang, P. Sirisomboon, Application of near infrared spectroscopy to detect aflatoxigenic fungal contamination in rice, Food Control 33 (2013) 207-214.

[94] P.-S. Liang, D.C. Slaughter, A. Ortega-Beltran, T.J. Michailides, Detection of fungal infection in almond kernels using near-infrared reflectance spectroscopy, Biosystems Engineering 137 (2015) 64-72.

[95] T. Phetkaeo, R. Klaithin, P. Theanjumpol, K. Kunasakdakul, S. Thanapornpoonpong, S. Vearasilp, Application of VIS/NIR spectroscopy to specify identity of Aspergillus flavus and Aspergillus niger isolated from maize seed, Agricultural Science Journal 42 (2011) 369-372.

[96] E. Durmus, A. Günes, H. Kalkan, Detection of aflatoxin and surface mould contaminated figs by using Fourier transform near-infrared reflectance spectroscopy, J Sci Food Agric 97 (2017) 317-323.

[97] W. Wang, G.W. Heitschmidt, X. Ni, W.R. Windham, S. Hawkins, X. Chu, Identification of aflatoxin B1 on maize kernel surfaces using hyperspectral imaging, Food Control 42 (2014) 78-86.

[98] W. Wang, G.W. Heitschmidt, W.R. Windham, P. Feldner, X. Ni, X. Chu, Feasibility of Detecting Aflatoxin B1 on Inoculated Maize Kernels Surface using Vis/NIR Hyperspectral Imaging, Journal of Food Science 80 (2015) M116-M122.

[99] W. Wang, K.C. Lawrence, X. Ni, S.-C. Yoon, G.W. Heitschmidt, P. Feldner, Near-infrared hyperspectral imaging for detecting Aflatoxin B1 of maize kernels, Food Control 51 (2015) 347-355.

[100] W. Wang, X. Ni, K.C. Lawrence, S.-C. Yoon, G.W. Heitschmidt, P. Feldner, Feasibility of detecting Aflatoxin B1 in single maize kernels using hyperspectral imaging, Journal of Food Engineering 166 (2015) 182-192.

[101] F. Zhu, H. Yao, Z. Hruska, R. Kincaid, R. Brown, D. Bhatnagar, T. Cleveland, Visible near-infrared

(VNIR) reflectance hyperspectral imagery for identifying aflatoxin-contaminated corn kernels, 2015 ASABE Annual International Meeting (2015), New Orleans, Louisiana, July 26-29, Paper number, 152189995.

[102] X. Chu, W. Wang, S.-C. Yoon, X. Ni, G.W. Heitschmidt, Detection of aflatoxin B1 (AFB1) in individual maize kernels using short wave infrared (SWIR) hyperspectral imaging, Biosystems Engineering 157 (2017) 13-23.

[103] L.M. Kandpal, S. Lee, M.S. Kim, H. Bae, B.-K. Cho, Short wave infrared (SWIR) hyperspectral imaging technique for examination of aflatoxin B1 (AFB1) on corn kernels, Food Control 51 (2015) 171-176.

[104] H. Yao, Z. Hruska, R. Kincaid, R.L. Brown, T.E. Cleveland, Differentiation of toxigenic fungi using hyperspectral imagery, Sens. & Instrumen. Food Qual. 2 (2008) 215-224.

[105] J. Jin, L. Tang, Z. Hruska, H. Yao, Classification of toxigenic and atoxigenic strains of Aspergillus flavus with hyperspectral imaging, Computers and Electronics in Agriculture 69 (2009) 158-164.

[106] A.D. Fiore, M. Reverberi, A. Ricelli, F. Pinzari, S. Serranti, A.A. Fabbri, G. Bonifazi, C. Fanelli, Early detection of toxigenic fungi on maize by hyperspectral imaging analysis, International Journal of Food Microbiology 144 (2010) 64-71.

[107] X. Zhao, W. Wang, X. Chu, C. Li, D. Kimuli, Early Detection of *Aspergillus parasiticus* Infection in Maize Kernels Using Near-Infrared Hyperspectral Imaging and Multivariate Data Analysis, Appl. Sci. 7 (2017) doi:10.3390/app7010090

[108] M.A. Teena, A. Manickavasagan, L. Ravikanth, D.S. Jayas, Near infrared (NIR) hyperspectral imaging to classify fungal infected date fruits, Journal of Stored Products Research 59 (2014) 306-313.

[109] K. Kheiralipour, H. Ahmadi, A. Rajabipour, S. Rafiee, M. Javan-Nikkhah, D.S. Jayas, K. Siliveru, Detection of fungal infection in pistachio kernel by long-wave near-infrared hyperspectral imaging technique, Quality Assurance and Safety of Crops & Foods 8 (2015) 129-135.

[110] K. Karuppiah, T. Senthilkumar, D.S. Jayas, N.D.G. White, Detection of fungal infection in five

different pulses using nearinfrared hyperspectral imaging, Journal of Stored Products Research 65 (2016) 13-18.

Figure Captions

Figure 1. Chemical structures of aflatoxins: (a) AFB_1, (b) AFB_2, (c) AFG_1, (d) AFG_2.

Figure 2. Mean fluorescence emission spectra of control and contaminated corn with aflatoxin threshold of (A) 20 µg/kg, (B) 100 µg/kg [62].

Figure 3. Scatter plots created by the first two canonical discriminant scores derived from normalized spectra of FT-NIRS of corn kernels [46].

Figure 4. Plots of mean absorbance spectra of *A. flavus*-infected corn kernels from different categories [86].

Figure 5. Mean spectra of infected (solid line) and uninfected (dashed line) almonds: (A) original absorbance spectra, (B) 2nd derivative absorbance spectra [94].

Figure 6. Contamination map of the PLS-DA model for corn samples [103].

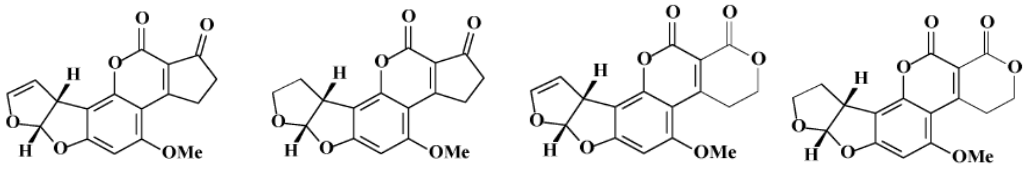

(a) (b) (c) (d)

Figure 1. Chemical structures of aflatoxins: (a) AFB_1, (b) AFB_2, (c) AFG_1, (d) AFG_2.

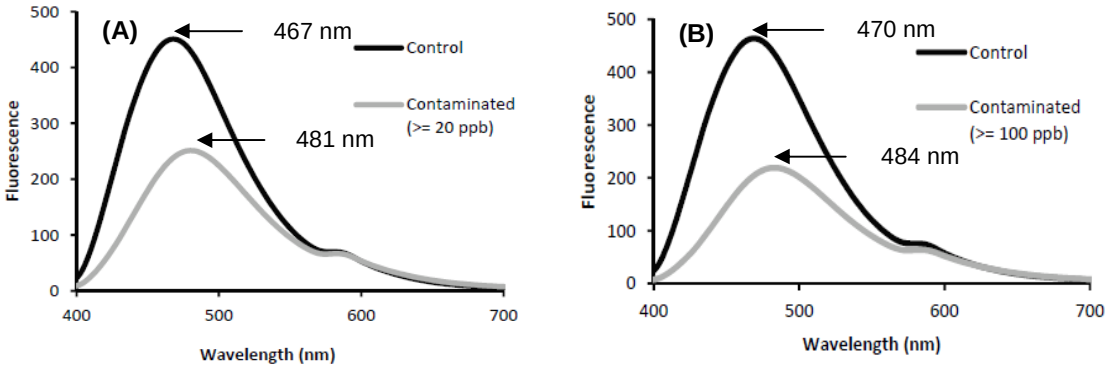

Figure 2. Mean fluorescence emission spectra of control and contaminated corn with aflatoxin threshold of (A) 20 µg/kg, (B) 100 µg/kg [62].

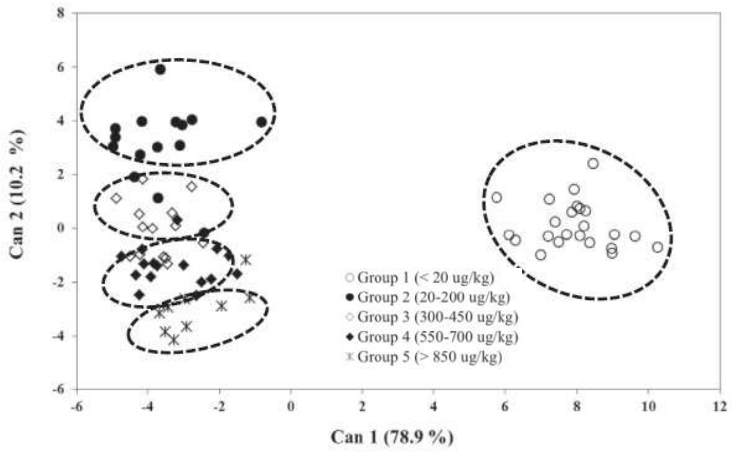

Figure 3. Scatter plots created by the first two canonical discriminant scores derived from normalized spectra of FT-NIRS of corn kernels [46].

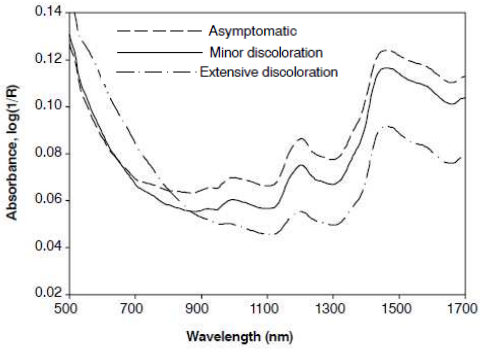

Figure 4. Plots of mean absorbance spectra of *A. flavus*-infected corn kernels from different categories [86].

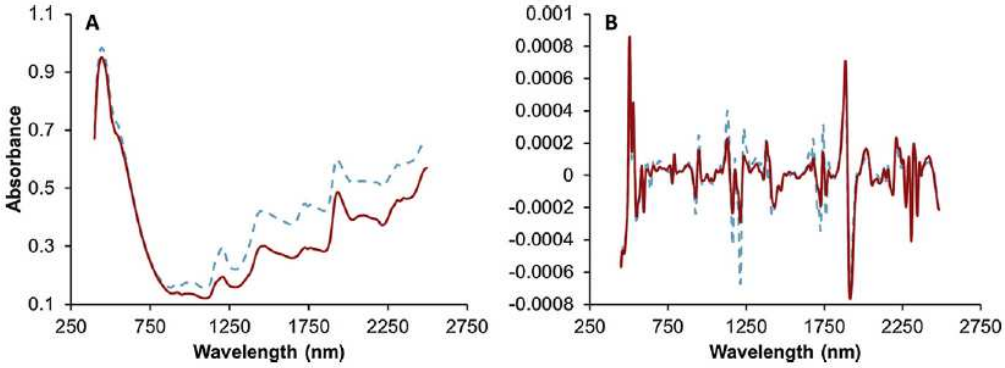

Figure 5. Mean spectra of infected (solid line) and uninfected (dashed line) almonds: (A) original absorbance spectra, (B) 2nd derivative absorbance spectra [94].

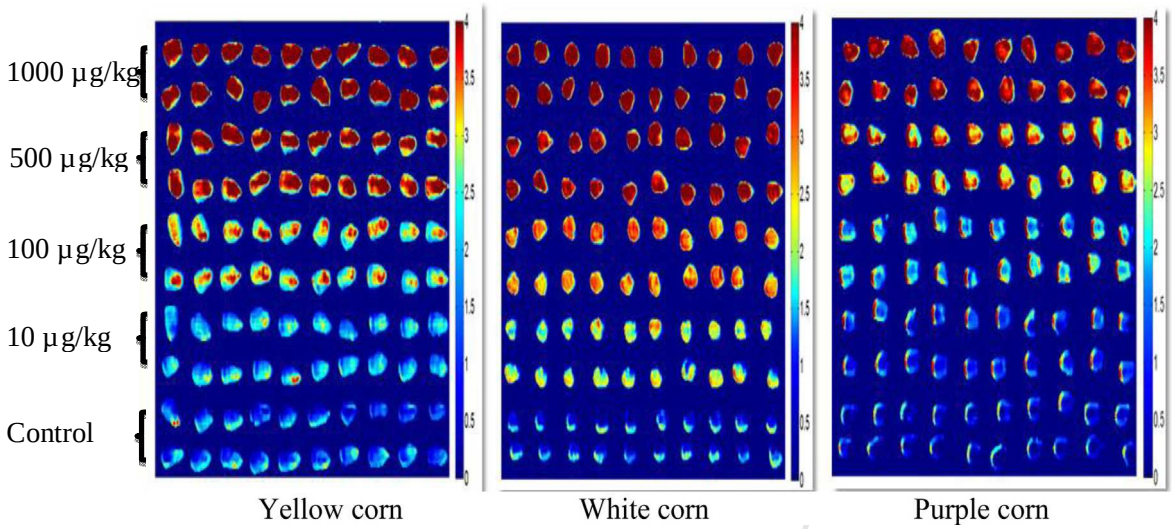

Figure 6. Contamination map of the PLS-DA model for corn samples [103].

Table 1. Recent publications on qualitative/quantitative detection of aflatoxin contamination in different agricultural products using the three optical methods.

Product	Tested aflatoxin	Contaminated sample source	Whether needs sample pre-processing before collecting spectral data?	Instrument used	Measurement mode	Spectral range (nm)	Data analysis method	Accuracy	Reference
Pistachio nut	Total aflatoxins	Provided by nut processor	No	Fluorescence MSI	Fluorescence	410, 440, 480, 520, 560, and 600	FSP-DF	92%	[39]
Cashew	Total aflatoxins	Provided by nut processor	No	Fluorescence MSI	Fluorescence	410, 440, 480, 520, 560, and 600	FSP-DF	82%	[39]
Red chili powder	AFB_1	Spiking with the AFB_1 standard in methanol	No	FT-NIRS	Diffuse reflectance	780-2500 (12800-3600 cm^{-1})	PLSR	R_P=0.967	[45]
Corn	Total aflatoxins	Both naturally contaminated and field-inoculated	Yes	FT-NIRS	Reflectance	1000-2500 (4000-9999 cm^{-1})	LDA, KNN, PLS-DA; MLR	Classification: 60-96% in validation; Quantification: R_P^2: 0.60-0.88, RMSEP: 106-194 µg/kg	[46]
Corn, barley, corn+barley	AFB_1	Induced by vaporization with water	No	Vis/NIRS	Reflectance	400-2500	PLS-DA	R_{CV}^2=0.80/0.85/0.92; SECV=0.211/0.176/0.142 for corn, barley and corn+barley, respectively	[47]
Corn, barley, corn+barley	AFB_1	Induced by vaporization with water	No	FT-NIRS	Reflectance	1112-2500 (9000-4000 cm^{-1})	PLS-DA	R_{CV}^2=0.82/0.84/0.81; SECV=0.201/0.183/0.203 for corn, barley and corn+barley, respectively	[47]
Corn	Total aflatoxins	Artificial inoculation of corn ears with *A. flavus* in the field	No	Fluorescence HSI	Fluorescence	400-600	SAM	86% with 20 ppb as the threshold; 88% with 100 ppb as the threshold	[58]
Corn	Total aflatoxins	Artificial inoculation of corn ears with *A. flavus* in the field	No	Fluorescence HSI	Fluorescence	400-600	MLR/DA	Adjusted R_C^2=0.72; classification accuracies: 84-91%	[59]
Corn	Total aflatoxins	Artificial inoculation of corn ears with *A. flavus* in the field	No	Fluorescence HSI	Fluorescence	400-600	GA-SPCR, PCR	R_C: 0.80-0.82	[60]
Corn	Total aflatoxins	Artificial inoculation of corn ears with *A. flavus* in the field	No	Fluorescence HSI	Fluorescence	400-600	GA-SVM	87.7% with 20 ppb as the threshold; 90.5% with 100 ppb as the threshold	[61]
Corn	Total aflatoxins	Artificial inoculation of corn ears with *A. flavus* in the field	No	Fluorescence HSI	Fluorescence	400-900	ML and binary encoding	Validation accuracy: 80-88%	[62]
Corn	Total aflatoxins	Artificial inoculation of corn ears with	No	Fluorescence HSI	Fluorescence	400-700	LDA	78.9 and 77.2% with 20 ppb as the threshold; 94.4 and 91.7%	[63]

		AF13 and AF38 in the field						with 100 ppb as the threshold	
Corn	Total aflatoxins	Artificial inoculation of corn ears with *A. flavus* in the field	No	Fluorescence HSI	Fluorescence	398.77-700.82	LS-SVM/KNN	86.67-93.33%	[65]
Corn	Total aflatoxins	Artificial inoculation of corn ears with *A. flavus* in the field	No	HSI	Reflectance	460.87-876.99	LS-SVM/KNN	90-94%	[65]
Corn	Total aflatoxins	Artificial inoculation of corn ears with *A. flavus* in the field	No	Fluorescence and normal HSI	Fluorescence and reflectance	Fluorescence: 398.77-700.82 Reflectance: 460.87-876.99	LS-SVM/KNN	90-95.33%	[65]
Peanut kernel	AFB_1	Inoculation with *A. flavus* and then incubation	Yes	Luminescence spectrometer	Fluorescence	400-600	/	R_C=-0.99 between $\log_{10}$ (AFB_1 concentration) and $\log_{10}$ (fluorescence intensity)	[66]
Hazelnut kernel	Total aflatoxins	Soaking in *A. parasiticus* suspension and pure water, and then incubation	No	Fluorescence MSI	Fluorescence	400-510, 550, 600	LDB-LDA	92.3%	[67]
Ground red chili pepper	Total aflatoxins	Obtained from the market	No	Fluorescence MSI	Fluorescence	400-510, 550, 600	LDB-LDA	79.2%	[67]
Pistachio nut	Total aflatoxins	/	No	Dual-wavelength fiber optic photometer	Fluorescence	420, 490	Log_{10} (I_{490}/I_{420})	Total classification errors of 20.4, 15.4, 4.0, and 13.9%	[70]
Nutmeg powder	AFB_1, AFB_2, AFG_1 and AFG_2	Uncontaminated samples spiked with aflatoxin standard	Yes	FF	Fluorescence	200-800	PLSR	R_P^2=0.773, SEP=1.0 μg/L,	[76]
Wheat	AFB_1	Purchased from markets	Yes	Spectrofluorimetry	Enhanced fluorescence	390-490	PARAFAC	R_C>0.99, LOD=0.9 μg/kg	[77]
Pistachio	AFB_1	Provided by a research lab	Yes	Spectrofluorimetry	Enhanced fluorescence	Normal: 380-480; Synchronous: 300-430	MLR, PCR, PLSR	REP: 4.35-27.95%	[78]
Ground red chili pepper	Total aflatoxins	Obtained from market	No	Fluorescence MSI	Fluorescence	400-510, 550, 600	LDA/MLP	67.5-87.5%	[83]
Ground red chili pepper flakes	Total aflatoxins	Obtained from market	No	Fluorescence HSI	Fluorescence	400-720	LDA/MLP/SVM	The best classification accuracy=72.63%	[83]
Ground red chili pepper flakes	Total aflatoxins	Obtained from market	No	HSI	Reflectance	400-720	LDA/MLP/SVM	The best classification accuracy=83.26%	[83]
Corn	Total aflatoxins	Wound-inoculation with *A. flavus* in the field	No	Vis/NIR spectrometer	Transmittance /Reflectance	Transmittance: 500-950, Reflectance: 550-1700	DA, PLSR	Classification accuracy>95% for groups of aflatoxins>100 or <10 ppb; ~25% for 10≤afaltoxins≤100 ppb	[84]
Corn	Total aflatoxins	Wound-inoculation with *A. flavus* in the	No	Vis/NIR spectrometer	Reflectance	400-1700	MD	> 99% with kernels stationary and 100 ppb as the threshold	[85]

		field or naturally infected							
Corn	Total aflatoxins	Wound-inoculation with *A. flavus* in the field or naturally infected	No	High-speed optical sorter	Reflectance	750, 1200	Rejection threshold	Reduction in aflatoxins averaged 82% with an initial level of aflatoxins at >10 ppb; 38% at <10 ppb	[85]
Corn	Total aflatoxins	Purchased from markets and artificial inoculation with *A. flavus* in the field	No	MS optical sorter	Reflectance	Nine distinct wavelengths between 470 and 1550	LDA	83% reduction in total aflatoxins	[87]
Paddy rice	AFB_1	Naturally and artificially contaminated by adding water to the samples induce the AFB_1 production	Yes	FT-NIRS	Reflectance	1000-2500 (4000-10000 cm^{-1})	PLSR	R_P^2: 0.79-0.85, SEP: 3.21-3.62 μg/kg	[88]
Red paprika powder	AFB_1, Total aflatoxins	Naturally contaminated	No	NIRS	Reflectance	1100-2000	modified PLSR	RMSEP=0.2/1.2 μg/kg for AFB_1/total aflatoxins	[89]
Corn	AFB_1	Artificial surface contamination with aflatoxin standard dissolved in methanol	No	HSI	Reflectance	1000-2500	Stepwise FDA	88%	[97]
Corn	AFB_1	Artificial surface contamination with aflatoxin standard dissolved in methanol	No	HSI	Reflectance	400-1000	Stepwise FDA	98%	[98]
Corn	AFB_1	Artificial inoculation of corn ears with *A. flavus* in the field	No	HSI	Reflectance	1000-2500	SAM	92.3%	[99]
Corn	AFB_1	Artificial inoculation of corn ears with *A. flavus* in the field	No	HSI	Reflectance	1000-2500	SAM	50-96.15%	[100]
Corn	Total aflatoxins	Artificial inoculation of corn ears with *A. flavus* in the field	No	HSI	Reflectance	400-900	DT	90%	[101]
Corn	Total aflatoxins	Artificial inoculation of corn ears with *A. flavus* in the field	No	HSI	Reflectance	700, 800	Pixel threshold based on ratio image	80%	[101]
Corn	AFB_1	Artificial inoculation of corn ears with *A. flavus* in the field	No	HSI	Reflectance	1000-2500	SVM, Correlation analysis	82.50%, R_P^2=0.70	[102]
Corn	AFB_1	Artificial surface contamination with AFB_1 solutions	No	HSI	Reflectance	1100-1700	PLS-DA	90.7-96.9%	[103]

Table 2. Recent publications on detection of aflatoxigenic fungal infection in different agricultural products using the three optical methods.

Product	Infected sample source	Instrument used	Measurement mode	Spectral range (nm)	Data analysis	Accuracy	Reference
Hazelnut kernel	Soaking in *A. parasiticus* suspension and pure water, and then incubation	Fluorescence MSI	Fluorescence	400-510, 550, 600	LDB-LDA	95.7%	[67]
Corn	Artificial inoculation of corn ears with *A. flavus* in the field	Vis/NIRS	Reflectance	550-1770	Stepwise DA	97-98% in identifying the "asymptomatic" samples; 85-91% in identifying the "extensive discoloration" samples	[86]
Corn	Artificial inoculation of corn ears with *A. flavus* in the field	MSI	Transmittance	780, 830, 870, 880, 890, 905, 920, 930, 960, 980 and 1020	Stepwise DA	93% and 90% achieved for asymptomatic and "extensive discoloration" groups, respectively	[86]
Peanut	Artificial inoculation with *A. flavus* between the two seed leaves	Spectrophotometer	Transmittance	700, 1100	Transmittance ration threshold	Aflatoxin content reduced to 4-18% levels after segragation	[90]
Corn	Wound-inoculation with *A. flavus* in the field	NIRS	Reflectance	904-1685	LDA, ANN	LDA: 93%, 76% and 74%, ANN: 81%, 86% and 68% for uninfected, early and advanced stage groups, respectively	[91]
Corn	Artificial inoculation with *A. flavus* and incubation	NIRS	Reflectance	1100-2500	PLSR	RPD: 1.55-1.74 for whole grain in determining the infected ratios; RPD: 3.40-5.36 for ground grain in determining the infected ratios	[92]
Rice	Artificial inoculation with different concentrations of *A. flavus* without incubation	NIRS	Reflectance	950-1650	PLSR	The best R_P and SEP are 0.71 and 28.07% for predicting the percentage of total fungal infection, respectively	[93]
Rice	Artificial inoculation with different concentrations of *A. flavus* without incubation	NIRS	Reflectance	950-1650	PLSR	The best R_P and SEP are 0.48 and 17.93% for predicting the percentage of yellow-green *Aspergillus* infection, respectively	[93]
Shelled almond kernel	Artificial inoculation with *A. flavus*, *A. parasiticus*, and incubation	NIRS	Reflectance	800-2500	CDA	The best and smallest classifiers achieved total classification error rates of 0.09% and 0.26%, respectively	[94]
Dried fig	Obtained from a fig co-operative	FT-NIRS	Reflectance	780-2500	LDC, LOGLC, QDC, KNN, PARZENC	Classification errors: 0.00-0.33%	[96]
Corn	Artificial inoculation with *A. flavus*, *A. parasiticus*, *A. niger* and incubation for different times	HSI	Reflectance	400-1000	Fisher's least significant difference analysis	The categories of uninoculated and day-2 infected samples already showed significant differences at 410 or 470 nm	[106]
Corn	Artificial inoculation with *A. parasiticus* and incubation for different times	HSI	Reflectance	921-2529	SVM	67.71-91.67%	[107]
Date fruit	Artificial inoculation with *A. flavus*	HSI	Reflectance	960-1700	LDA, QDA	LDA for classifying UC/SC and different stages of IS samples: 74-97%/74-94%;	[108]

						QDA for classifying UC/SC and different stages of IS samples: 97-100%/95-100%;	
Pistachio kernel	Artificial inoculation with *A. flavus* KK11 and R5	HSI	Reflectance	900-1700	LDA, QDA	LDA accuracies in 15-class classification: 45.8-97.9%; QDA accuracies in 15-class classification: 70.8-100%; QDA accuracies in classifying healthy, samples infected by *A. flavus* KK11 or R5 at all stages: 91.3-100%	[109]
Five pulses of chick peas, green peas, lentils, pinto beans and kidney beans	Artificial inoculation with *A. flavus* and incubation	HSI	Reflectance	900-1700	LDA, QDA	LDA accuracies in 6-class classification: 71.6-100%; QDA accuracies in 6-class classification: 69.1-100%	[110]

- Key optical methods for detecting aflatoxin and fungal contamination
- Advantages of optical techniques over conventional detection methods
- Advances in optical method development for aflatoxin and fungal contamination
- Applications of optical methods in reducing aflatoxin contamination of commodities
- Future trends and challenges for detection of aflatoxin and fungal contamination